Analyst

PAPER

Cite this: *Analyst*, 2020, **145**, 6910

Multimodal imaging of biological tissues using combined MALDI and NAPA-LDI mass spectrometry for enhanced molecular coverage†

Jarod A. Fincher,[a] Andrew R. Korte,*[a] Sridevi Yadavilli,[b] Nicholas J. Morris[c] and Akos Vertes*[a]

Received 25th April 2020,
Accepted 18th August 2020

DOI: 10.1039/d0an00836b

rsc.li/analyst

Mass spectrometry imaging (MSI) is a powerful analytical technique that enables detection, discovery, and identification of multiple classes of biomolecules, while simultaneously mapping their spatial distributions within a sample (*e.g.*, a section of biological tissue). The limitation in molecular coverage afforded by any single MSI platform has led to the development of multimodal approaches that incorporate two or more techniques to obtain greater chemical information. Matrix-assisted laser desorption ionization (MALDI) is a preeminent ionization technique for MSI applications because the wide range of available matrices allows some degree of enhancement with respect to the detection of particular molecular classes. Nonetheless, MALDI has a limited ability to detect and image several classes of molecules, *e.g.*, neutral lipids, in complex samples. Laser desorption ionization from silicon nanopost arrays (NAPA-LDI or NAPA) has been shown to offer complementary coverage with respect to MALDI by providing improved detection of neutral lipids and some small metabolites. Here, we present a multimodal imaging method in which a single tissue section is consecutively imaged at low and high laser fluences, generating spectra that are characteristic of MALDI and NAPA ionization, respectively. The method is demonstrated to map the distributions of species amenable to detection by MALDI (*e.g.*, phospholipids and intermediate-mass metabolites) and NAPA (*e.g.*, neutral lipids such as triglycerides and hexosylceramides, and small metabolites) in mouse brain and lung tissue sections.

1. Introduction

Mass spectrometry imaging (MSI) is becoming a useful tool in histology and drug discovery due to its ability to spatially map diverse biomolecules, including metabolites, lipids, peptides, and proteins, in tissue sections without the need for chemical labeling.[1–5] For example, MSI has been used for the classification of tumor subtypes, and to identify tumor margins between cancerous and noncancerous tissue regions.[6–10] In addition, spatial mapping of drug candidates, pharmaceuticals and the corresponding metabolites has been demonstrated, even achieving absolute quantitation in some cases.[11–14] Currently, matrix-assisted laser desorption ionization (MALDI) is a top method for MSI due to its relative simplicity, broad molecular coverage, and wide availability of the required instrumentation. The impressive molecular coverage provided by MALDI can, in part, be attributed to the large array of available matrices, with many of them providing preferential ionization of different biomolecular classes.[15–17]

While MSI provides detailed chemical information, in most configurations it cannot match the spatial resolution afforded by optical microscopy. Moreover, the chemical information provided by an MSI experiment varies significantly depending upon the chosen sample preparation and ionization technique. To overcome these limitations, methodologies have been developed in which two or more imaging techniques are combined to provide complementary information. In the most common implementation of this approach, a tissue section is collected from the region immediately adjacent to the section subjected to MSI, and is designated for histological staining, *e.g.*, by hematoxylin and eosin (H&E), and imaging by optical microscopy. Image fusion allows for the combination of

---

[a] *Department of Chemistry, The George Washington University, Washington, DC 20052, USA. E-mail: vertes@gwu.edu, andrew.r.korte@gmail.com*
[b] *Research Center for Genetic Medicine, Children's National Medical Center, Washington, DC 20010, USA*
[c] *UES, Inc., Beavercreek, OH 45432, USA*

† Electronic supplementary information (ESI) available. See DOI: 10.1039/d0an00836b

optical images of histologically stained tissues (high spatial resolution and low chemical specificity) with MSI-generated chemical images (lower spatial resolution and high chemical specificity) to infer molecular distributions at higher spatial resolutions than typically achieved by MSI alone.[18] Considerable effort is being directed toward developing multimodal imaging platforms that combine two or more MSI ionization modalities. For example, MALDI has been combined with secondary ion mass spectrometry (SIMS) or desorption electrospray ionization (DESI), and imaging of the same tissue section by MALDI in positive and negative ion mode has been demonstrated.[19–21] MALDI-MSI images have also been co-registered with autofluorescence and magnetic resonance imaging (MRI) to provide complementary information.[22,23]

Although MALDI offers excellent molecular coverage in MSI, in complex samples it exhibits low ionization efficiency for some small metabolites and for neutral lipids, such as triglycerides (TGs) and hexosylceramides (HexCers). The detection of neutral lipids is hindered by ion suppression effects induced by phospholipids, for example, phosphatidylcholines (PCs).[24–26] To circumvent these limitations, several novel LDI methods utilizing a large variety of nanomaterials and nanostructures have been developed.[27] For example, silver or gold nanoparticles provide remarkably higher ionization efficiencies for TGs.[28–31] In the recently developed MALDI-2 technique, a second laser intercepts the desorption plume for post-ionization, resulting in significantly enhanced sensitivity and the detection of less abundant species. This was shown to greatly improve the molecular coverage of neutral lipid species and phospholipids, as well as often difficult to detect sterols and pharmaceuticals.[32–35]

Comparing MALDI with LDI from silicon nanopost arrays (NAPA),[36] a matrix-free MS platform, has been shown to provide complementary coverage for metabolites.[37,38] Molecular imaging of biological samples has also been demonstrated by NAPA-MSI.[39] A remarkable difference between the fluence dependence of the two ionization methods is the significantly lower ionization threshold for MALDI compared to LDI from NAPA.[40] This presents an opportunity for the combination of these two techniques to study the same tissue section by both MSI modalities. Compared to MALDI, enhanced ionization efficiency was observed by LDI from NAPA for neutral lipid classes such as TGs and HexCers, whereas for phospholipids MALDI exhibited higher ion yields.[41–43] Thus, a combined method is expected to provide broader molecular coverage compared to the two techniques performed separately.

Here we present a new multimodal imaging approach that combines the ionization capabilities afforded by the MALDI- and NAPA-LDI-MSI platforms to obtain improved molecular coverage in imaging of a single tissue section (see Fig. 1). This is made possible, in large part, by the significantly different laser fluence needed for ion production by the two platforms. For the combined technique, a tissue section is thaw-mounted on top of the nanofabricated silicon posts in the NAPA chip, and a thin layer of MALDI matrix is applied to the surface of this sample. In the first MSI pass, a relatively low laser fluence is applied to generate MALDI spectra. At this laser fluence the NAPA structure below the tissue section does not contribute to ion production. In the second MSI pass, a comparatively high laser fluence is applied to deposit enough energy into the underlying nanoposts to induce desorption and ionization. The utility of the combined method is demonstrated on MSI of mouse brain and lung tissue sections.

2. Experimental

2.1 Chemicals

Solvents methanol (catalog no. A452-4) and water (catalog no. W6-212) were purchased at LC-MS grade from Fisher Scientific (Hampton, NH). Matrices 9-aminoacridine (9-AA, catalog no. 92817) and α-cyano-4-hydroxycinnamic acid (CHCA, catalog no. C8982) for MALDI were purchased from Sigma-Aldrich (St Louis, MO).

2.2 Fabrication of NAPA imaging chips

The detailed process for the nanofabrication of NAPA imaging chips has been described in a previous publication.[44] Briefly, silicon nanoposts were produced with a periodicity of 337 nm and post dimensions of 1100 nm in height and 150 nm in diameter optimized for maximum ion yield by LDI. NAPA imaging chips were fabricated from low-resistivity p-type silicon wafers (Silicon Valley Microelectronics, Inc., Santa Clara, CA) by methods utilizing deep ultraviolet projection lithography (DUV-PL) followed by deep reactive ion etching (DRIE). The size of a typical imaging NAPA chip was 25 × 25 mm^2.

2.3 Sample preparation for MSI

Whole mouse brains and mouse lungs were provided by Children's National Medical Center (Washington, DC) in accordance with the protocol approved by the Institutional Animal Care and Use Committee (IACUC). All tissue samples were stored at −80 °C until preparation for MSI analysis, whereupon they were placed into a pre-chilled cryomicrotome (CM1800, Leica Microsystems Inc., Nussloch, Germany) at −25 °C and allowed to equilibrate for 30 min before sectioning. Both mouse brain and mouse lung tissue samples were sectioned at 10 μm thickness and immediately thaw-mounted onto NAPA imaging chips and placed in a vacuum desiccator for 30 min.

Matrix deposition was performed using an in-house built oscillating capillary nebulizer. Briefly, an Aztek A470 airbrush (Testors, Vernon Hills, IL) was modified to accommodate a fused silica capillary threaded through the spray nozzle. Matrix solution was fed through the capillary by means of a syringe (1750TLL, Hamilton Co., Reno, NV) and a syringe pump (KS100, KD Scientific, Holliston, MA). The airbrush nozzle was positioned ∼23 cm above the tissue surface and spraying was driven by nitrogen as the nebulizing gas at a pressure of 276 kPa (40 psi). For lung imaging experiments, a 20 mg mL^{-1}

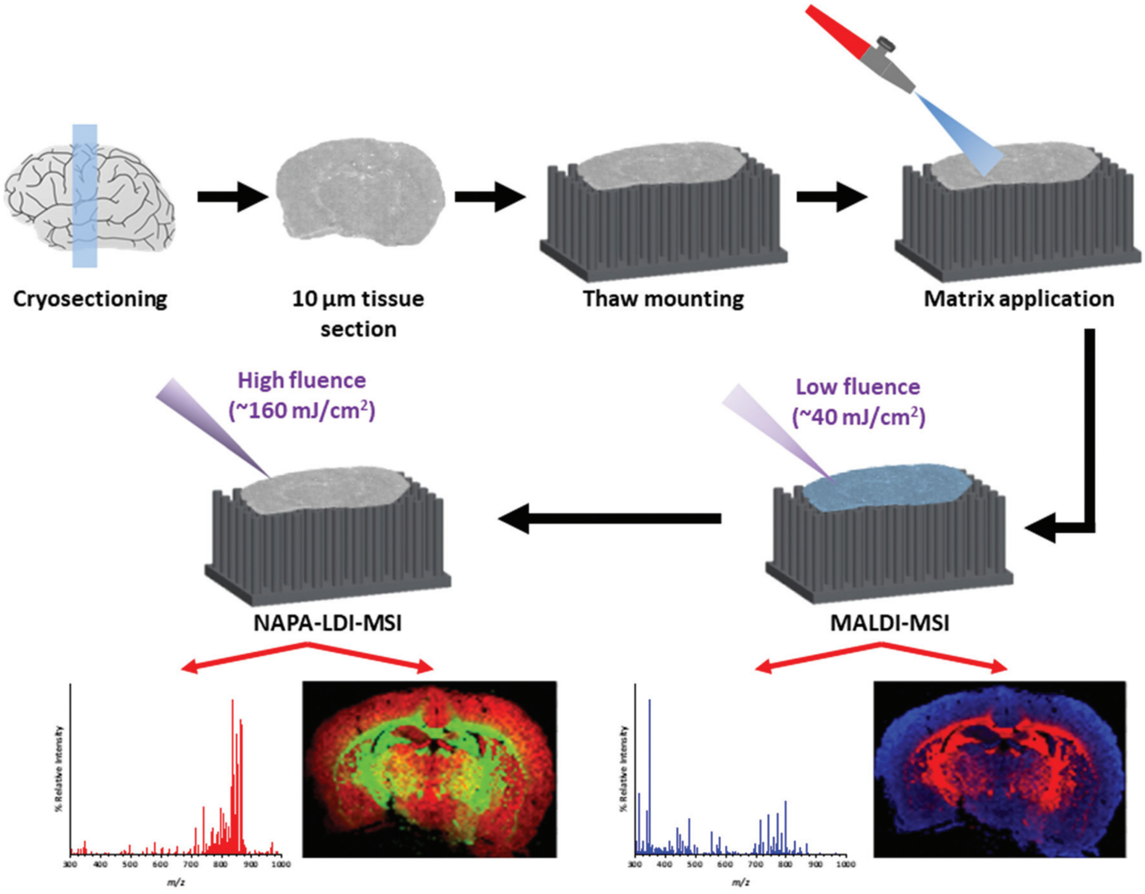

Fig. 1 Simplified schematic demonstrating multimodal imaging of a single tissue section by MALDI- and NAPA-LDI-MSI. The MALDI pass is performed at ~40 mJ cm^{-2}, whereas for the NAPA pass the laser is operated at ~160 mJ cm^{-2}. Chemical images shown in this illustration present different lipid species detected with similar spatial distributions using the two different platforms and are intended to help illustrate the application workflow.

solution of CHCA in methanol was sprayed at a flow rate of 50 µL min^{-1}, with a total sprayed volume of 300 µL. For brain imaging experiments, a 10 mg mL^{-1} solution of 9-AA in methanol was sprayed at 50 µL min^{-1}, with a total sprayed volume of 300 µL.

2.4 Data acquisition and analysis

All MSI data for mouse brain and mouse lung tissue samples were acquired on a MALDI-LTQ-Orbitrap XL mass spectrometer equipped with a nitrogen laser emitting radiation at 337 nm with a 60 Hz repetition rate and a focal spot size of ~80 µm × 100 µm (Thermo Scientific, San Jose, CA). The laser was operated at fluences in the 40–50 mJ cm^{-2} range with 10 shots per scan for MALDI (MALDI pass) and in the 140–200 mJ cm^{-2} range with 3 shots per scan for NAPA (NAPA pass). In the MALDI pass most of the matrix material was removed from the tissue surface at the focal spot. Thus, in the MALDI pass, no ions were generated by LDI from NAPA, and in the NAPA pass, ion production was dominated by the NAPA-LDI process. Imaging data was collected with a modest lateral resolution of 100 µm, well below what was achievable by either of the methods.[39] All MSI experiments were run at a mass resolving power setting of 30 000 with an m/z range of 500 to 1000. Reproducibility of NAPA-LDI-MSI has been demonstrated for biological applications, including the same type of mouse brain and lung tissues.[41,43] Well-controlled matrix application is a critical factor for reproducible MALDI-MSI. It is achievable by several matrix application methods, including the one used in this study.[45]

All imaging data were processed by importing the raw data files (*.raw) into ImageQuest (Thermo Scientific, San Jose, CA), whereby chemical images were generated with a mass tolerance of ≤5 mDa. In order to co-register the chemical images generated by the MALDI pass and the NAPA pass, chemical images were exported out of ImageQuest and imported into ImageJ, a freely available image processing software.[46] The images were then overlaid using the alignment of two color channels. Lipid ions were tentatively identified by matching measured m/z values to a previously assembled in-house reference list with mass accuracy tolerance of $\Delta m/z \leq \pm 5$ mDa. For mouse brain and lung tissues, this list had been compiled based on UPLC-MS/MS measurements.[41,43] Putative lipid assignments for this work can be found in the ESI.†

3. Results and discussion

To demonstrate multimodal imaging using the combination of MALDI and NAPA-LDI, a 10 μm thick mouse brain tissue section was thaw-mounted onto a NAPA imaging chip and placed in a vacuum desiccator for ~30 min. The dehydrated tissue section was spray coated by 9-AA matrix using the oscillating capillary nebulizer built in house. First, MALDI-MSI was performed at a low laser fluence (~40 mJ cm^{-2}) in negative ion mode, allowing detection and imaging of lipid classes such as sulfatides (STs) and phosphatidylinositols (PIs) (see the top image panels in Fig. 2). The number of laser pulses for each spot in this MALDI pass was selected to remove most of the matrix material from the tissue surface. Observing the depletion of the matrix signal indicated that ten laser pulses per spot was sufficient to achieve this condition. In general, this number depends on the nature of the matrix and the applied laser fluence. In the MALDI pass, medium-size metabolites including UDP-ribose, ADP-ribose, and oxidized glutathione were also detected. Immediately upon the completion

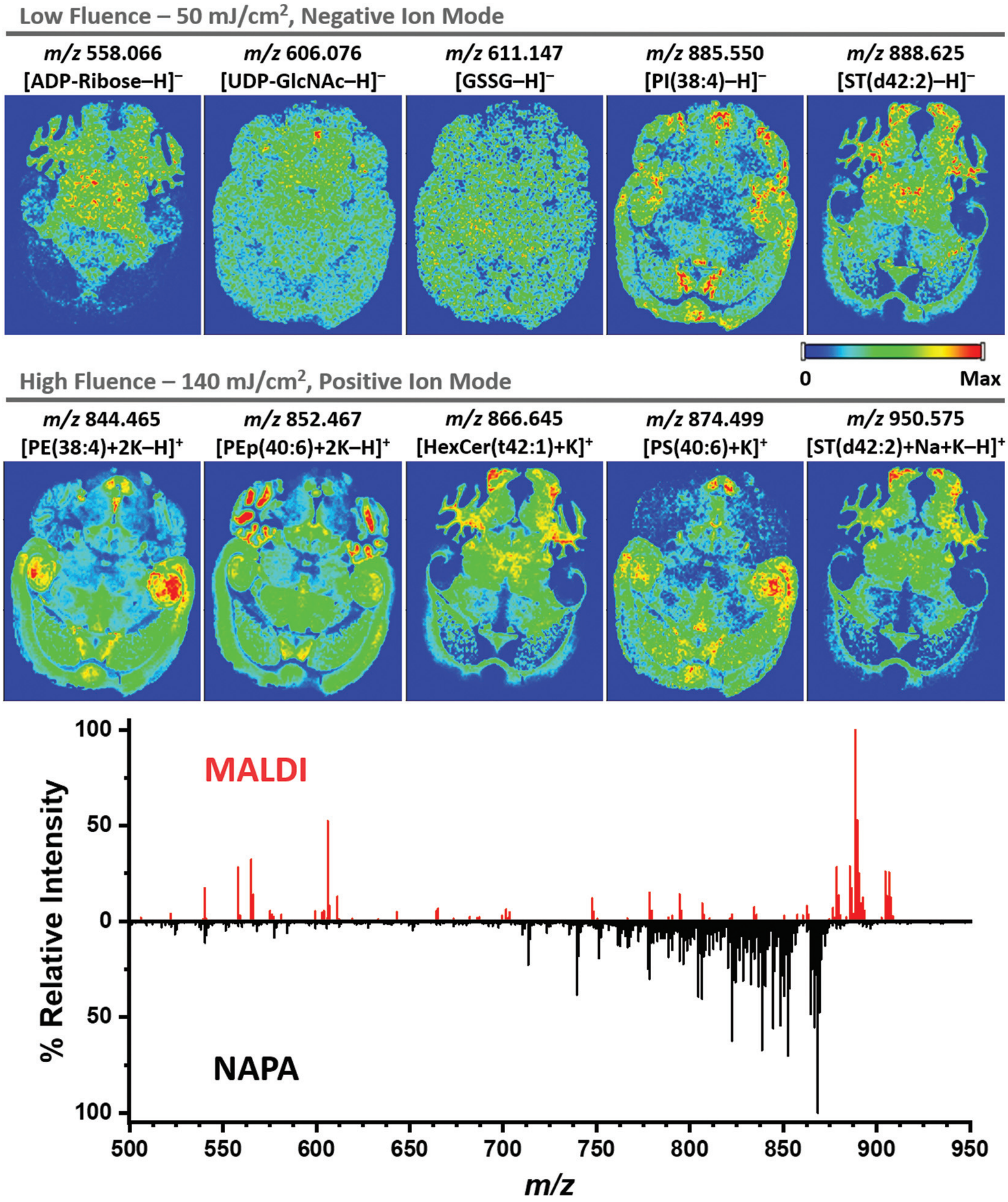

Fig. 2 Ion distribution images showing spectral intensities for specific *m/z* values throughout a section of mouse brain tissue. Images at the top were generated from low fluence negative mode data in a MALDI pass, whereas images in middle panels were produced from high fluence positive mode data collected in a NAPA pass. Acquisitions were performed consecutively on the same tissue section. In the bottom panel, comparison of mass spectra is shown averaged over approximately the entire tissue area for the MALDI- and NAPA-LDI-MSI acquisitions.

of the MALDI imaging acquisition, the same tissue section was re-imaged in positive ion mode at a considerably higher laser fluence (~160 mJ cm^{-2}) by NAPA-LDI, whereby phosphatidylethanolamines (PEs), phosphatidylethanolamine plasmalogens (PEps), and HexCers among other molecular species were selectively ionized and detected (see image panels in the middle in Fig. 2). Comparison of the integrated mass spectra for the MALDI pass and the NAPA pass in the bottom panel of Fig. 2 illustrates the complementary nature of the two ionization techniques. An extensive tentative identification list for the detected ions in mouse brain tissue section is presented in Table S1 of the ESI.†

The complementary molecular coverages of these two platforms have been evaluated and discussed in detail in previous work.[37,41,43] In brief, unlike MALDI, NAPA has been shown to efficiently ionize neutral lipid species, such as HexCers TGs, as well as PE plasmalogens. In contrast, MALDI has been proven superior at efficiently ionizing phospholipid species, such as PCs and SMs in positive ion mode, as well as STs and PIs in negative ion mode. Additionally, the lower internal energy of MALDI-generated ions is more conducive for the detection of thermally labile compounds like ADP-ribose and glutathione. Indeed, whereas MALDI generates ions with lower but matrix dependent internal energy, the ions produced from NAPA exhibit a higher, laser fluence and polarization dependent internal energy.[47,48]

The ability to reimage the same tissue by the two ionization techniques relies on the observation that laser exposure in MALDI only consumes the matrix material and does not remove most of the underlying tissue. As the matrix solution droplets are deposited on the sample surface, they dissolve some components of the tissue and upon drying matrix-analyte co-crystallization occurs. Laser exposure of these crystals in the MALDI pass gives rise to the MALDI signal, and upon multiple exposures the matrix crystals are almost completely removed from the interrogated tissue surface. In the NAPA pass, the laser radiation traverses through the exposed tissue and the underlying silicon nanoposts absorb the laser pulse energy. The rapidly heating nanoposts induce the volatilization of the tissue at the tips of the posts, and field enhancement at these same tips results in efficient ionization.

Additional capabilities of the combined MALDI and NAPA-LDI MSI method were tested on an alternative tissue sample. A 10 μm thick mouse lung tissue section was thaw-mounted onto a NAPA imaging chip as described above. The tissue was coated with CHCA MALDI matrix. In a departure from the brain imaging experiments, the lung tissue was imaged in positive ion mode by both techniques. First, MALDI-MSI was performed at a lower laser fluence (~40 mJ cm^{-2}). This was immediately followed by re-imaging of the same tissue section at higher laser fluence (~200 mJ cm^{-2}) by NAPA-LDI. As seen in Fig. 3, phospholipids such as phosphatidylcholines (PCs) were selectively ionized in the MALDI pass at reduced laser fluence. When re-imaging the same tissue at higher laser fluence in the NAPA pass, TGs and PEs were selectively ionized. A tentative identification list for the detected ions in the mouse lung tissue section is presented in Table S2 of the ESI.†

To demonstrate the complementary nature of the two imaging modalities, MALDI and NAPA-LDI images are compared for the same ions in the top and middle row of panels in Fig. 3, respectively. Distributions for PC ions at *m*/*z* 756.558 ($[PC(34:3) + H]^+$) and *m*/*z* 780.553 ($[PC(36:5) + H]^+$) are clearly revealed by the MALDI pass (see the two left panels in the top row in Fig. 3), whereas the NAPA pass (see the two left panels in the middle row in Fig. 3) does not provide discernable patterns. Conversely, for *m*/*z* 780.496 ($[PE(36:3) + K]^+$) and *m*/*z* 879.742 ($[TG(52:3) + Na]^+$) the MALDI pass resulted in weak to no signal (see the two right panels in the top row in Fig. 3), whereas the NAPA pass produced detailed distributions (see the two right panels in the middle row in Fig. 3). This complementarity is also illustrated by the mass spectra integrated for the MALDI and NAPA-LDI images (see the bottom panel in Fig. 3).

As seen in Fig. 4, the acquisition of MALDI and NAPA images from the same tissue section allows for detection and imaging of lipid classes that are not typically detected using a single MSI platform or ion polarity. This circumvents the need for the preparation of multiple consecutive sample sections, eliminating concerns about variability in sample treatment and tissue heterogeneity. Given the incompatibility of MS imaging with typical tissue fixation techniques, preparation of highly similar consecutive sections is non-trivial. Moreover, the typical tissue section thickness (~10 μm) is on the order of the size of most animal cells, so the chemical similarity of consecutive sections cannot be assured.

The use of the same tissue section for the two techniques also simplifies image processing. In these experiments, imaging in both modalities was performed using the same instrument position file and there was no need to identify fiducial markers for coregistration. In the brain imaging presented here, overlaying images for *m*/*z* 885.550 (detected by negative ion mode MALDI and identified as $[PI(38:4) - H]^-$) and *m*/*z* 866.645 (detected by positive ion mode NAPA and identified as $[HexCer(t42:1) + K]^+$) revealed complementary distributions, with localization to the gray and white matter, respectively. Similarly, *m*/*z* 888.625 (MALDI, identified as $[ST(d42:2) - H]^-$) localized to the white matter and *m*/*z* 852.467 (NAPA, identified as $[PEp(40:6) + 2K - H]^+$) localized to the gray matter were found to have complementary spatial distributions. Overlaying cross-platform lung tissue images also revealed complementary localizations among PCs, TAGs, and PEs (see Fig. S1 in the ESI†).

The ability of the dual imaging platform presented here to detect a range of biomolecules presents numerous potential applications. For example, many of the species shown in Fig. 2, 3 and 4 are implicated in important biological processes or disease progression. Reduced glutathione (shown in its oxidized form (GSSG) in the top panel of Fig. 2) is the predominant antioxidant in brain tissue, and plays a crucial role in protecting nervous tissue from oxidative damage that has been implicated in neurological diseases such as Alzheimer's disease and Parkinson's disease.[49] Furthermore, PE lipids have been shown to be associated with Alzheimer's disease, where

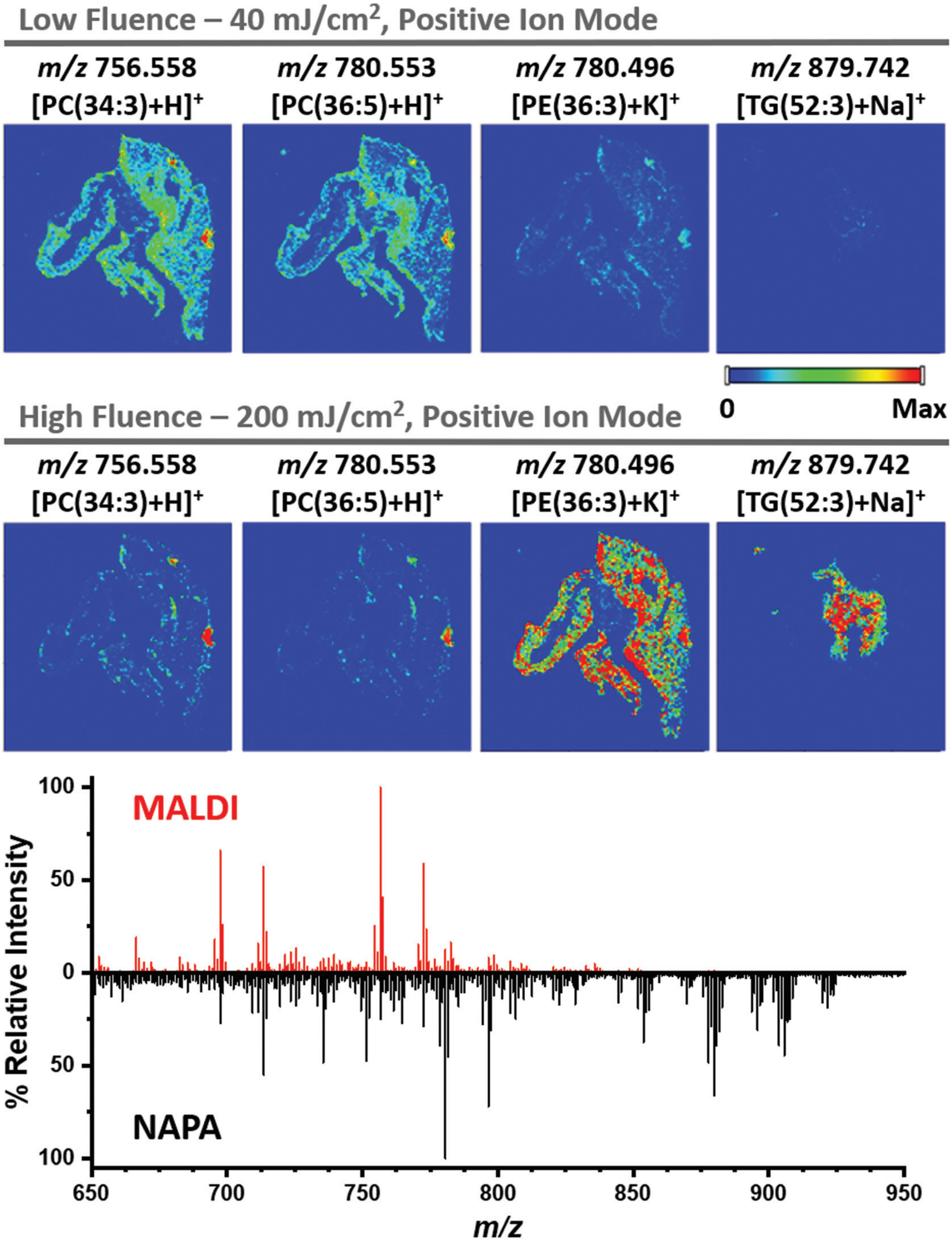

Fig. 3 Images showing ion intensity distributions throughout a section of mouse lung tissue. Images in the top row were generated by a low laser fluence (40 mJ cm^{-2}) MALDI pass, whereas images in the middle row were generated by a high laser fluence (200 mJ cm^{-2}) NAPA pass. All data was collected in positive ion mode. Acquisitions were performed consecutively on the same tissue section. The bottom panel shows the comparison of mass spectra averaged over approximately the entire tissue area for the MALDI- and NAPA-LDI-MSI acquisitions.

they were found to be significantly decreased in diseased tissue.[50] ADP-ribose (see its distribution in the top panel in Fig. 2) is known to be involved in repair of DNA damage.[51] Within the brain, sulfatides (distributions are shown in the middle and top panels of Fig. 2 and the left panel of Fig. 4) and HexCers (see distributions in the middle panel of Fig. 2 and the center panel of Fig. 4) are critical to the development of the myelin sheath. They also factor into many forms of extracellular binding, including bacterial and viral infection.[52] PIs (demonstrated in the top and left panels of Fig. 2 and 4, respectively) exist in a vast multitude of forms and isomers, and a recent review has extensively discussed their roles in cel-

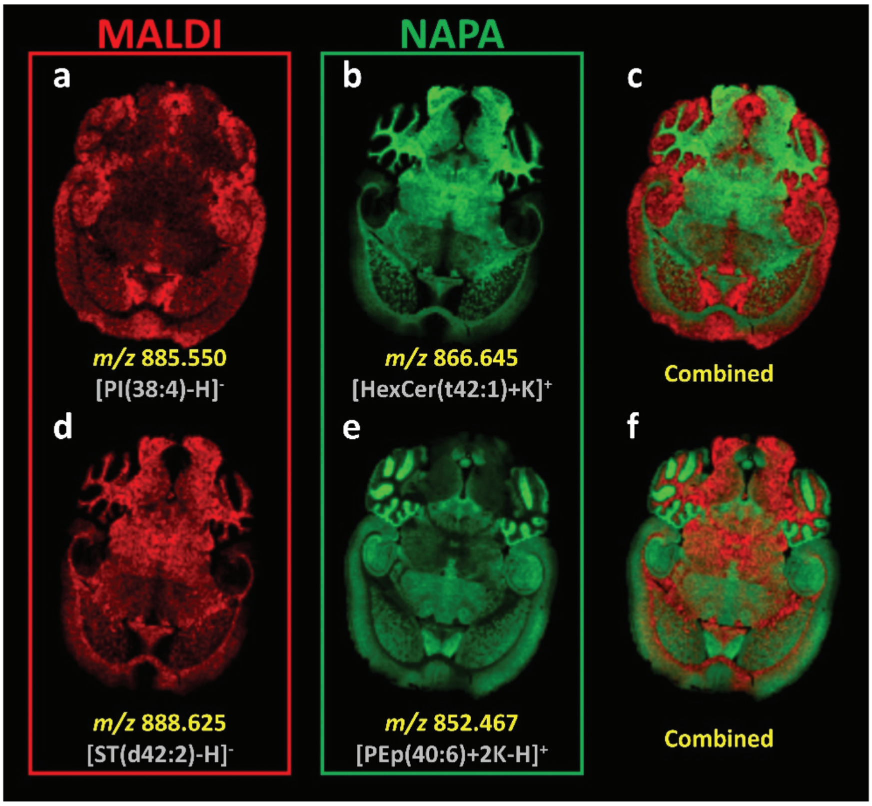

Fig. 4 Overlaid chemical images from consecutive MALDI- and NAPA-LDI-MSI analysis of the same mouse brain tissue section. Images were overlaid using ImageJ software.

lular signaling and disease.[53] In breast cancer tissue samples, PCs (examples are depicted in the top panel of Fig. 3) were detected at significantly higher levels, allowing for differentiation between cancerous and non-cancerous tissue types.[54] Lastly, increased levels of TGs (shown in the middle panel of Fig. 3) have been associated with life-altering diseases like type-2 diabetes and coronary heart disease.[55–57]

4. Conclusions

The multimodal imaging platform based on the combination of MALDI and NAPA-LDI has been demonstrated for imaging of chemical species in mouse brain and lung tissues and can be applied to other sample types. In these experiments, the consecutive use of MALDI- and NAPA-LDI-MSI allowed for the detection and imaging of a range of chemical species, including several classes of lipids and small molecule metabolites. Although the high fluences required for NAPA-LDI-MSI are typically destructive to the tissue sample, we envision that multiple MALDI imaging analyses (*e.g.* in different polarities) can be performed prior to a final NAPA-LDI-MSI step. This dual imaging capability offers enhanced molecular coverage in MSI experiments, providing enriched information on spatial variations or temporal changes in lipid composition. For example, this multimodal imaging platform could be used to investigate host–pathogen interactions, an area of research where MSI has already provided insight into inflammatory signaling pathways with respect to lipids and microbial pathogenesis.[58,59]

Ethical statement

All experiment were performed in accordance with the guidelines of IACUC and approved by the IACUC.

Conflicts of interest

There are no conflicts to declare.

Acknowledgements

Research was sponsored by the U.S. Army Research Office and the Defense Advanced Research Projects Agency and was accomplished under Cooperative Agreement Number W911NF-14-2-0020. The views and conclusions contained in this document are those of the authors and should not be interpreted as representing the official policies, either expressed or implied, of the Army Research Office, DARPA, or the U.S. Government. The U.S. Government is authorized to reproduce and distribute reprints for Government purposes notwithstanding any copyright notation hereon.

The silicon NAPA structures used in this work were produced at the UC Santa Barbara Nanofabrication Facility, a part of the NSF funded National Nanotechnology Infrastructure Network.

References

1 R. M. Caprioli, T. B. Farmer and J. Gile, *Anal. Chem.*, 1997, **69**, 4751–4760.
2 R. W. Hutchinson, A. G. Cox, C. W. McLeod, P. S. Marshall, A. Harper, E. L. Dawson and D. R. Howlett, *Anal. Biochem.*, 2005, **346**, 225–233.
3 S. N. Jackson, M. Ugarov, T. Egan, J. D. Post, D. Langlais, J. A. Schultz and A. S. Woods, *J. Mass Spectrom.*, 2007, **42**, 1093–1098.
4 K. Chughtai and R. M. A. Heeren, *Chem. Rev.*, 2010, **110**, 3237–3277.
5 P. Nemes, A. S. Woods and A. Vertes, *Anal. Chem.*, 2010, **82**, 982–988.
6 L. S. Eberlin, I. Norton, A. L. Dill, A. J. Golby, K. L. Ligon, S. Santagata, R. G. Cooks and N. Y. R. Agar, *Cancer Res.*, 2012, **72**, 645–654.
7 S. Santagata, L. S. Eberlin, I. Norton, D. Calligaris, D. R. Feldman, J. L. Ide, X. H. Liu, J. S. Wiley, M. L. Vestal, S. H. Ramkissoon, D. A. Orringer, K. K. Gill, I. F. Dunn, D. Dias-Santagata, K. L. Ligon, F. A. Jolesz, A. J. Golby, R. G. Cooks and N. Y. R. Agar, *Proc. Natl. Acad. Sci. U. S. A.*, 2014, **111**, 11121–11126.
8 S. Kang, H. S. Shim, J. S. Lee, D. S. Kim, H. Y. Kim, S. H. Hong, P. S. Kim, J. H. Yoon and N. H. Cho, *J. Proteome Res.*, 2010, **9**, 1157–1164.
9 P. Chaurand, M. E. Sanders, R. A. Jensen and R. M. Caprioli, *Am. J. Pathol.*, 2004, **165**, 1057–1068.
10 J. Kriegsmann, M. Kriegsmann and R. Casadonte, *Int. J. Oncol.*, 2015, **46**, 893–906.
11 F. P. Y. Barre, M. R. L. Paine, B. Flinders, A. J. Trevitt, P. D. Kelly, R. Ait-Belkacem, J. P. Garcia, L. B. Creemers, J. Stauber, R. J. Vreeken, B. Cillero-Pastor, S. R. Ellis and R. M. A. Heeren, *Anal. Chem.*, 2019, **91**, 10840–10848.
12 J. G. Swales, G. Hamm, M. R. Clench and R. J. A. Goodwin, *Int. J. Mass Spectrom.*, 2019, **437**, 99–112.
13 J. M. Wiseman, D. R. Ifa, Y. X. Zhu, C. B. Kissinger, N. E. Manicke, P. T. Kissinger and R. G. Cooks, *Proc. Natl. Acad. Sci. U. S. A.*, 2008, **105**, 18120–18125.
14 B. M. Prentice, C. W. Chumbley and R. M. Caprioli, *J. Am. Soc. Mass Spectrom.*, 2017, **28**, 136–144.
15 M. C. Fitzgerald, G. R. Parr and L. M. Smith, *Anal. Chem.*, 1993, **65**, 3204–3211.
16 A. Thomas, J. L. Charbonneau, E. Fournaise and P. Chaurand, *Anal. Chem.*, 2012, **84**, 2048–2054.
17 A. R. Buchberger, K. DeLaney, J. Johnson and L. J. Li, *Anal. Chem.*, 2018, **90**, 240–265.
18 R. Van de Plas, J. H. Yang, J. Spraggins and R. M. Caprioli, *Nat. Methods*, 2015, **12**, 366–U138.
19 S. Chughtai, K. Chughtai, B. Cillero-Pastor, A. Kiss, P. Agrawal, L. MacAleese and R. M. A. Heeren, *Int. J. Mass Spectrom.*, 2012, **325**, 150–160.
20 L. S. Eberlin, X. H. Liu, C. R. Ferreira, S. Santagata, N. Y. R. Agar and R. G. Cooks, *Anal. Chem.*, 2011, **83**, 8366–8371.
21 S. R. Ellis, J. Cappell, N. O. Potocnik, B. Balluff, J. Hamaide, A. Van der Linden and R. M. A. Heeren, *Analyst*, 2016, **141**, 3832–3841.
22 N. H. Patterson, M. Tuck, R. Van de Plas and R. M. Caprioli, *Anal. Chem.*, 2018, **90**, 12395–12403.
23 A. S. Attia, K. A. Schroeder, E. H. Seeley, K. J. Wilson, N. D. Hammer, D. C. Colvin, M. L. Manier, J. J. Nicklay, K. L. Rose, J. C. Gore, R. M. Caprioli and E. P. Skaar, *Cell Host Microbe*, 2012, **11**, 664–673.
24 G. R. Asbury, K. Al-Saad, W. F. Siems, R. M. Hannan and H. H. Hill, *J. Am. Soc. Mass Spectrom.*, 1999, **10**, 983–991.
25 B. Emerson, J. Gidden, J. O. Lay Jr. and B. Durham, *J. Lipid Res.*, 2010, **51**, 2428–2434.
26 M. Petkovic, J. Schiller, M. Muller, S. Benard, S. Reichl, K. Arnold and J. Arnhold, *Anal. Biochem.*, 2001, **289**, 202–216.
27 J. A. Stolee, B. N. Walker, V. Zorba, R. E. Russo and A. Vertes, *Phys. Chem. Chem. Phys.*, 2012, **14**, 8453–8471.
28 M. Dufresne, J. F. Masson and P. Chaurand, *Anal. Chem.*, 2016, **88**, 6018–6025.
29 M. Dufresne, A. Thomas, J. Breault-Turcot, J.-F. Masson and P. Chaurand, *Anal. Chem.*, 2013, **85**, 3318–3324.
30 S. N. Jackson, K. Baldwin, L. Muller, V. M. Womack, J. A. Schultz, C. Balaban and A. S. Woods, *Anal. Bioanal. Chem.*, 2014, **406**, 1377–1386.
31 J. Son, G. Lee and S. Cha, *J. Am. Soc. Mass Spectrom.*, 2014, **25**, 891–894.
32 J. Soltwisch, H. Kettling, S. Vens-Cappell, M. Wiegelmann, J. Muthing and K. Dreisewerd, *Science*, 2015, **348**, 211–215.
33 S. R. Ellis, J. Soltwisch, M. R. L. Paine, K. Dreisewerd and R. M. A. Heeren, *Chem. Commun.*, 2017, **53**, 7246–7249.
34 M. Niehaus, J. Soltwisch, M. E. Belov and K. Dreisewerd, *Nat. Methods*, 2019, **16**, 925–931.
35 A. P. Bowman, J. F. J. Bogie, J. J. A. Hendriks, M. Haidar, M. Belov, R. M. A. Heeren and S. R. Ellis, *Anal. Bioanal. Chem.*, 2020, **412**, 2277–2289.
36 B. N. Walker, J. A. Stolee, D. L. Pickel, S. T. Retterer and A. Vertes, *J. Phys. Chem. C*, 2010, **114**, 4835–4840.
37 A. R. Korte, N. J. Morris and A. Vertes, *Anal. Chem.*, 2019, **91**, 3951–3958.
38 A. R. Korte, S. A. Stopka, N. Morris, T. Razunguzwa and A. Vertes, *Anal. Chem.*, 2016, **88**, 8989–8996.
39 S. A. Stopka, C. Rong, A. R. Korte, S. Yadavilli, J. Nazarian, T. T. Razunguzwa, N. J. Morris and A. Vertes, *Angew. Chem., Int. Ed.*, 2016, **55**, 4482–4486.
40 J. A. Stolee, B. N. Walker, Y. Chen and A. Vertes, in *International Symposium on High Power Laser Ablation 2010*, ed. C. R. Phipps, 2010, vol. 1278, pp. 98–110.
41 J. A. Fincher, J. E. Dyer, A. R. Korte, S. Yadavilli, N. J. Morris and A. Vertes, *J. Comp. Neurol.*, 2019, **527**, 2101–2121.

42 J. A. Fincher, D. R. Jones, A. R. Korte, J. E. Dyer, P. Parlanti, A. Popratiloff, C. A. Brantner, N. J. Morris, R. K. Pirlo, V. K. Shanmugam and A. Vertes, *Sci. Rep.*, 2019, **9**, 17508.

43 J. A. Fincher, A. R. Korte, J. E. Dyer, S. Yadavilli, N. J. Morris, D. R. Jones, V. K. Shanmugam, R. K. Pirlo and A. Vertes, *J. Mass Spectrom.*, 2020, **55**, e4443.

44 N. J. Morris, H. Anderson, B. Thibeault, A. Vertes, M. J. Powell and T. T. Razunguzwa, *RSC Adv.*, 2015, **5**, 72051–72057.

45 E. Gemperline, S. Rawson and L. J. Li, *Anal. Chem.*, 2014, **86**, 10030–10035.

46 C. A. Schneider, W. S. Rasband and K. W. Eliceiri, *Nat. Methods*, 2012, **9**, 671–675.

47 G. H. Luo, I. Marginean and A. Vertes, *Anal. Chem.*, 2002, **74**, 6185–6190.

48 J. A. Stolee and A. Vertes, *Phys. Chem. Chem. Phys.*, 2011, **13**, 9140–9146.

49 R. Dringen, *Prog. Neurobiol.*, 2000, **62**, 649–671.

50 R. B. Chan, T. G. Oliveira, E. P. Cortes, L. S. Honig, K. E. Duff, S. A. Small, M. R. Wenk, G. H. Shui and G. Di Paolo, *J. Biol. Chem.*, 2012, **287**, 2678–2688.

51 C. Liu, A. Vyas, M. A. Kassab, A. K. Singh and X. C. Yu, *Nucleic Acids Res.*, 2017, **45**, 8129–8141.

52 T. Takahashi and T. Suzuki, *J. Lipid Res.*, 2012, **53**, 1437–1450.

53 P. Raghu, A. Joseph, H. Krishnan, P. Singh and S. Saha, *Front. Mol. Neurosci.*, 2019, **12**, 208.

54 S. Guenther, L. J. Muirhead, A. V. M. Speller, O. Golf, N. Strittmatter, R. Ramakrishnan, R. D. Goldin, E. Jones, K. Veselkov, J. Nicholson, A. Darzi and Z. Takats, *Cancer Res.*, 2015, **75**, 1828–1837.

55 M. Adiels, S. O. Olofsson, M. R. Taskinen and J. Boren, *Arterioscler., Thromb., Vasc. Biol.*, 2008, **28**, 1225–1236.

56 G. S. Berenson, S. R. Srinivasan, W. H. Bao, W. P. Newman, R. E. Tracy, W. A. Wattigney and S. Bogaulas Heart, *N. Engl. J. Med.*, 1998, **338**, 1650–1656.

57 M. R. Taskinen, *Diabetologia*, 2003, **46**, 733–749.

58 A. J. Scott, J. M. Post, R. Lerner, S. R. Ellis, J. Lieberman, K. A. Shirey, R. M. A. Heeren, L. Bindila and R. K. Ernst, *Proc. Natl. Acad. Sci. U. S. A.*, 2017, **114**, 12596–12601.

59 J. L. Moore, R. M. Caprioli and E. P. Skaar, *Curr. Opin. Microbiol.*, 2014, **19**, 45–51.

Electronic Supplementary Information

for

Multimodal Imaging of Biological Tissues Using Combined MALDI and NAPA-LDI Mass Spectrometry for Enhanced Molecular Coverage

Jarod A. Fincher[1], Andrew R. Korte*[1], Sridevi Yadavilli[2], Nicholas J. Morris[3], and Akos Vertes*[1]

[1]*Department of Chemistry, The George Washington University, Washington, DC 20052, USA*

[2]*Research Center for Genetic Medicine, Children's National Medical Center, Washington, DC 20010, USA*

[3]*UES, Inc., Beavercreek, OH 45432, USA*

*Co-corresponding authors:

Akos Vertes

Email: vertes@gwu.edu

ORCID: 0000-0001-5186-5352

Andrew Korte

Email: andrew.r.korte@gmail.com

ORCID: 0000-0003-4270-966X

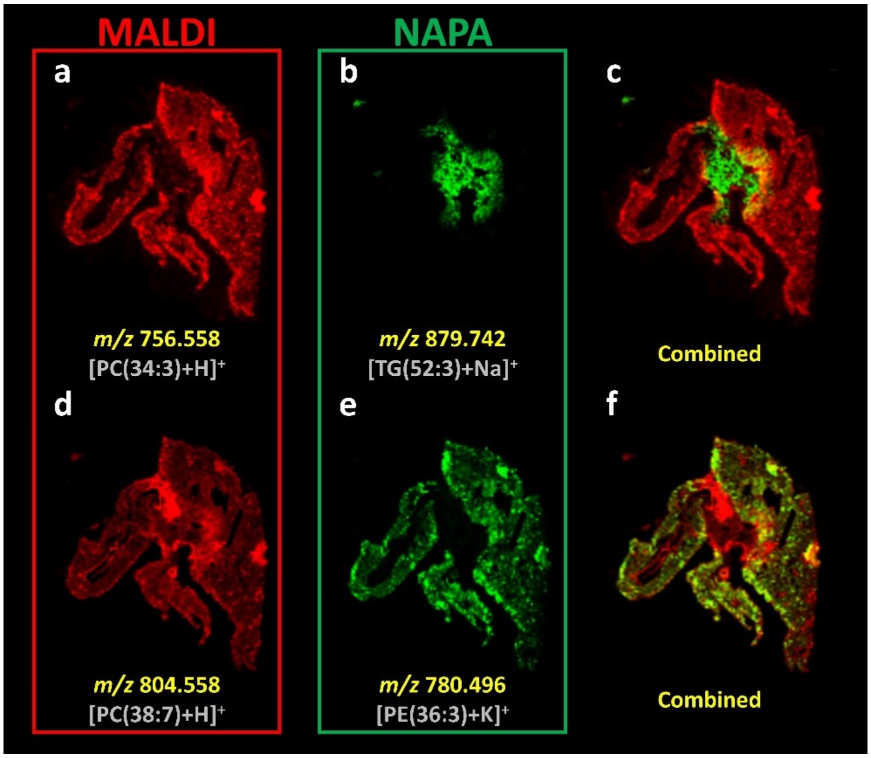

Figure S1. Overlaid chemical images from consecutive MALDI- and NAPA-LDI-MSI analysis of the same mouse lung tissue section. Images were overlaid using ImageJ software.

Table S1. Tentative lipid identifications based on mass accuracy tolerance of Δ*m/z* ≤ ±5 mDa from analysis of mouse brain tissue sections analyzed by MALDI- and NAPA-LDI-MSI. For *m/z* values with multiple potential interpretations, all possibilities are listed.

Sample	Meas. *m/z*	Calc. *m/z*	Δm (mDa)	Tentative identification
Brain_MALDI	305.1283	305.1280	0.3	[|FA(14:0)|+2K-H]+
Brain_MALDI	319.1434	319.1436	-0.2	[|FA(15:0)|+2K-H]+
Brain_MALDI	331.1441	331.1436	0.5	[|FA(16:1)|+2K-H]+
Brain_MALDI	333.1593	333.1593	0.0	[|FA(16:0)|+2K-H]+
Brain_MALDI	361.1899	361.1906	-0.7	[|FA(18:0)|+2K-H]+
Brain_MALDI	369.3516	369.3516	0.0	[|Cholesterol (-H2O)|+H]+
Brain_MALDI	496.3403	496.3398	0.5	[|LysoPC(16:0)|+H]+
Brain_MALDI	530.2020	530.2046	-2.6	[|LysoPE(16:0)|+2K-H]+
Brain_MALDI	570.2576	570.2567	0.9	[|LysoPE(22:6)|+2Na-H]+
Brain_MALDI	666.4839	666.4833	0.6	[|CerP(d18:1/18:1)|+Na]+
Brain_MALDI	682.4577	682.4572	0.4	[|CerP(d18:1/18:1)|+K]+
Brain_MALDI	697.4787	697.4803	-1.6	[|PA(36:4)|+H]+
Brain_MALDI	697.4787	697.4779	0.9	[|PA(34:1)|+Na]+
Brain_MALDI	709.4198	709.4205	-0.7	[|PA(34:3)|+K]+
Brain_MALDI	713.4518	713.4518	0.0	[|PA(34:1)|+K]+
Brain_MALDI	723.4941	723.4935	0.6	[|PA(36:2)|+Na]+
Brain_MALDI	723.4941	723.4959	-1.8	[|PA(38:5)|+H]+
Brain_MALDI	725.3930	725.3921	1.0	[|PA(32:0)|+2K-H]+
Brain_MALDI	725.5105	725.5116	-1.1	[|PA(38:4)|+H]+
Brain_MALDI	725.5105	725.5092	1.3	[|PA(36:1)|+Na]+
Brain_MALDI	725.5577	725.5568	0.9	[|SM(d34:1)|+Na]+
Brain_MALDI	735.4351	735.4362	-1.0	[|PA(36:4)|+K]+
Brain_MALDI	737.4536	737.4518	1.8	[|PA(36:3)|+K]+
Brain_MALDI	739.4095	739.4101	-0.6	[|DG(40:9)|+2K-H]+
Brain_MALDI	739.4680	739.4675	0.5	[|PA(36:2)|+K]+
Brain_MALDI	741.4858	741.4831	2.6	[|PA(36:1)|+K]+
Brain_MALDI	741.5313	741.5307	0.5	[|SM(d34:1)|+K]+
Brain_MALDI	745.4787	745.4755	3.2	[|PA(36:2)|+2Na-H]+
Brain_MALDI	745.4787	745.4779	0.8	[|PA(38:5)|+Na]+
Brain_MALDI	745.4787	745.4803	-1.6	[|PA(40:8)|+H]+
Brain_MALDI	748.5858	748.5851	0.8	[|PE(36:0)|+H]+
Brain_MALDI	750.5834	750.5854	-2.1	[|HexCer(d36:1)|+Na]+
Brain_MALDI	751.4083	751.4077	0.6	[|PA(34:1)|+2K-H]+
Brain_MALDI	751.5263	751.5272	-1.0	[|PA(40:5)|+H]+
Brain_MALDI	751.5263	751.5248	1.4	[|PA(38:2)|+Na]+
Brain_MALDI	753.5892	753.5881	1.1	[|SM(d36:1)|+Na]+
Brain_MALDI	753.5892	753.5905	-1.3	[|SM(d38:4)|+H]+
Brain_MALDI	756.5525	756.5538	-1.3	[|PC(34:3)|+H]+

Sample	Meas. *m/z*	Calc. *m/z*	Δm (mDa)	Tentative identification
Brain_MALDI	760.5863	760.5851	1.2	[|PC(34:1)|+H]+
Brain_MALDI	761.4521	761.4518	0.3	[|PA(38:5)|+K]+
Brain_MALDI	762.6020	762.6007	1.2	[|PC(34:0)|+H]+
Brain_MALDI	763.4684	763.4675	1.0	[|PA(38:4)|+K]+
Brain_MALDI	765.4848	765.4831	1.7	[|PA(38:3)|+K]+
Brain_MALDI	766.5527	766.5511	1.5	[|CerP(d42:2)|+K]+
Brain_MALDI	767.4991	767.4988	0.3	[|PA(38:2)|+K]+
Brain_MALDI	769.5627	769.5620	0.7	[|SM(d36:1)|+K]+
Brain_MALDI	770.5087	770.5097	-0.9	[|PC(32:1)|+K]+
Brain_MALDI	770.5087	770.5071	1.6	[|PE 36:3p|+2Na-H]+
Brain_MALDI	770.5087	770.5095	-0.8	[|PE 38:6p|+Na]+
Brain_MALDI	772.5263	772.5228	3.5	[|PE 36:2p|+2Na-H]+
Brain_MALDI	772.5263	772.5252	1.1	[|PE 38:5p|+Na]+
Brain_MALDI	774.6010	774.6007	0.2	[|PE(38:1)|+H]+
Brain_MALDI	775.5296	775.5272	2.4	[|PA(42:7)|+H]+
Brain_MALDI	777.4249	777.4234	1.5	[|PA(36:2)|+2K-H]+
Brain_MALDI	778.4766	778.4784	-1.8	[|PE(36:4)|+K]+
Brain_MALDI	779.4410	779.4390	2.0	[|PA(36:1)|+2K-H]+
Brain_MALDI	780.4936	780.4940	-0.4	[|PE(36:3)|+K]+
Brain_MALDI	782.5682	782.5694	-1.3	[|PC(36:4)|+H]+
Brain_MALDI	782.5682	782.5670	1.1	[|PC(34:1)|+Na]+
Brain_MALDI	783.4582	783.4573	0.9	[|PG(34:3)|+K]+
Brain_MALDI	784.5271	784.5253	1.8	[|PE(36:1)|+K]+
Brain_MALDI	784.5838	784.5851	-1.3	[|PC(36:3)|+H]+
Brain_MALDI	784.5838	784.5827	1.1	[|PC(34:0)|+Na]+
Brain_MALDI	785.4527	785.4518	0.9	[|PA(40:7)|+K]+
Brain_MALDI	787.4675	787.4675	0.0	[|PA(40:6)|+K]+
Brain_MALDI	789.4830	789.4831	-0.1	[|PA(40:5)|+K]+
Brain_MALDI	794.4509	794.4499	1.0	[|PE(34:1)|+2K-H]+
Brain_MALDI	796.4674	796.4656	1.9	[|PE(34:0)|+2K-H]+
Brain_MALDI	796.5262	796.5253	0.9	[|PC(34:2)|+K]+
Brain_MALDI	796.5262	796.5228	3.5	[|PE 38:4p|+2Na-H]+
Brain_MALDI	797.5939	797.5933	0.5	[|SM(d38:1)|+K]+
Brain_MALDI	798.5422	798.5410	1.2	[|PC(34:1)|+K]+
Brain_MALDI	798.5422	798.5408	1.4	[|PE 40:6p|+Na]+
Brain_MALDI	798.5422	798.5384	3.8	[|PE 38:3p|+2Na-H]+
Brain_MALDI	800.4376	800.4393	-1.8	[|PE 36:4p|+2K-H]+
Brain_MALDI	800.5591	800.5589	0.2	[|PE 42:8p|+H]+
Brain_MALDI	800.5591	800.5566	2.4	[|PC(34:0)|+K]+
Brain_MALDI	800.5591	800.5565	2.6	[|PE 40:5p|+Na]+
Brain_MALDI	801.4240	801.4234	0.7	[|PA(38:4)|+2K-H]+
Brain_MALDI	802.4796	802.4784	1.2	[|PE(38:6)|+K]+

Sample	**Meas. *m/z***	**Calc. *m/z***	**Δm (mDa)**	**Tentative identification**
Brain_MALDI	804.4904	804.4940	-3.6	[|PE(38:5)|+K]+
Brain_MALDI	804.5524	804.5538	-1.4	[|PC(38:7)|+H]+
Brain_MALDI	804.5524	804.5514	1.0	[|PC(36:4)|+Na]+
Brain_MALDI	804.5524	804.5490	3.4	[|PC(34:1)|+2Na-H]+
Brain_MALDI	806.5102	806.5097	0.5	[|PE(38:4)|+K]+
Brain_MALDI	808.4655	808.4656	0.0	[|PC(32:1)|+2K-H]+
Brain_MALDI	808.5828	808.5851	-2.3	[|PC(38:5)|+H]+
Brain_MALDI	808.5828	808.5827	0.1	[|PC(36:2)|+Na]+
Brain_MALDI	809.6512	809.6507	0.5	[|SM(d40:1)|+Na]+
Brain_MALDI	810.5995	810.5983	1.2	[|PC(36:1)|+Na]+
Brain_MALDI	810.5995	810.6007	-1.2	[|PC(38:4)|+H]+
Brain_MALDI	813.4834	813.4831	0.2	[|PA(42:7)|+K]+
Brain_MALDI	814.5123	814.5148	-2.4	[|PE 40:6p|+K]+
Brain_MALDI	815.5184	815.5199	-1.5	[|PG(36:1)|+K]+
Brain_MALDI	816.4354	816.4343	1.2	[|PE(36:4)|+2K-H]+
Brain_MALDI	820.4668	820.4656	1.2	[|PE(36:2)|+2K-H]+
Brain_MALDI	820.5258	820.5253	0.5	[|PC(36:4)|+K]+
Brain_MALDI	820.5258	820.5228	3.0	[|PE 40:6p|+2Na-H]+
Brain_MALDI	822.4828	822.4812	1.6	[|PE(36:1)|+2K-H]+
Brain_MALDI	822.4828	822.4868	-4.0	[|PI-Cer(d34:2)|+2Na-H]+
Brain_MALDI	822.6441	822.6430	1.1	[|HexCer(t40:1)|+Na]+
Brain_MALDI	824.4386	824.4393	-0.7	[|PE 38:6p|+2K-H]+
Brain_MALDI	824.5576	824.5566	1.0	[|PC(36:2)|+K]+
Brain_MALDI	824.5576	824.5565	1.1	[|PE 42:7p|+Na]+
Brain_MALDI	824.5576	824.5541	3.5	[|PE 40:4p|+2Na-H]+
Brain_MALDI	825.4227	825.4234	-0.6	[|PA(40:6)|+2K-H]+
Brain_MALDI	825.6266	825.6246	1.9	[|SM(d40:1)|+K]+
Brain_MALDI	826.5729	826.5723	0.6	[|PC(36:1)|+K]+
Brain_MALDI	826.5729	826.5721	0.8	[|PE 42:6p|+Na]+
Brain_MALDI	826.5729	826.5697	3.2	[|PE 40:3p|+2Na-H]+
Brain_MALDI	828.4945	828.4940	0.5	[|PE(40:7)|+K]+
Brain_MALDI	828.4945	828.4973	-2.8	[|PI-Cer(t33:0)|+2Na-H]+
Brain_MALDI	828.5555	828.5538	1.8	[|PC(40:9)|+H]+
Brain_MALDI	830.5104	830.5097	0.7	[|PE(40:6)|+K]+
Brain_MALDI	832.5838	832.5803	3.5	[|PC(36:1)|+2Na-H]+
Brain_MALDI	832.5838	832.5851	-1.3	[|PC(40:7)|+H]+
Brain_MALDI	832.5838	832.5827	1.1	[|PC(38:4)|+Na]+
Brain_MALDI	832.6648	832.6637	1.2	[|HexCer(d42:2)|+Na]+
Brain_MALDI	834.6819	834.6793	2.5	[|HexCer(d42:1)|+Na]+
Brain_MALDI	836.4959	836.4969	-0.9	[|PC(34:1)|+2K-H]+
Brain_MALDI	838.6170	838.6168	0.3	[|PI-Cer(38:0)|+H]+
Brain_MALDI	838.6170	838.6169	0.1	[|HexCer(t40:1)|+K]+

Sample	Meas. *m/z*	Calc. *m/z*	Δm (mDa)	Tentative identification
Brain_MALDI	840.4352	840.4343	0.9	[|PE(38:6)|+2K-H]+
Brain_MALDI	842.4534	842.4499	3.5	[|PE(38:5)|+2K-H]+
Brain_MALDI	844.4664	844.4656	0.8	[|PE(38:4)|+2K-H]+
Brain_MALDI	844.5269	844.5253	1.5	[|PC(38:6)|+K]+
Brain_MALDI	844.5269	844.5228	4.1	[|PE 42:8p|+2Na-H]+
Brain_MALDI	846.4681	846.4682	-0.1	[|PS(38:6)|+K]+
Brain_MALDI	846.5372	846.5384	-1.2	[|PE 42:7p|+2Na-H]+
Brain_MALDI	846.5372	846.5410	-3.8	[|PC(38:5)|+K]+
Brain_MALDI	848.5577	848.5541	3.7	[|PE 42:6p|+2Na-H]+
Brain_MALDI	848.5577	848.5566	1.1	[|PC(38:4)|+K]+
Brain_MALDI	848.6371	848.6376	-0.6	[|HexCer(d42:2)|+K]+
Brain_MALDI	850.6759	850.6743	1.6	[|HexCer(d42:1(2OH))|+Na]+
Brain_MALDI	856.5832	856.5803	2.9	[|PC(38:3)|+2Na-H]+
Brain_MALDI	856.5832	856.5827	0.5	[|PC(40:6)|+Na]+
Brain_MALDI	864.6331	864.6325	0.6	[|HexCer(d42:2(2OH))|+K]+
Brain_MALDI	866.4502	866.4499	0.3	[|PE(40:7)|+2K-H]+
Brain_MALDI	866.6493	866.6482	1.1	[|HexCer(d42:1(2OH))|+K]+
Brain_MALDI	866.6493	866.6481	1.2	[|PI-Cer(40:0)|+H]+
Brain_MALDI	868.4669	868.4656	1.3	[|PE(40:6)|+2K-H]+
Brain_MALDI	872.4980	872.4969	1.2	[|PE(40:4)|+2K-H]+
Brain_MALDI	872.5578	872.5566	1.2	[|PC(40:6)|+K]+
Brain_MALDI	874.5015	874.4995	2.0	[|PS(40:6)|+K]+
Brain_MALDI	912.4572	912.4554	1.8	[|PS(40:6)|+2K-H]+
Brain_MALDI	912.6398	912.6429	-3.1	[|PC(42:3)|+2Na-H]+
Brain_MALDI	963.4779	963.4762	1.7	[|PI(38:4)|+2K-H]+
Brain_NAPA	333.1594	333.1593	0.1	[|FA(16:0)|+2K-H]+
Brain_NAPA	369.3516	369.3516	0.0	[|Cholesterol (-H2O)|+H]+
Brain_NAPA	381.1585	381.1593	-0.8	[|FA(20:4)|+2K-H]+
Brain_NAPA	405.1594	405.1593	0.1	[|FA(22:6)|+2K-H]+
Brain_NAPA	502.2702	502.2696	0.7	[|Carnitine(18:1)|+2K-H]+
Brain_NAPA	544.2193	544.2202	-1.0	[|LysoPC(14:0)|+2K-H]+
Brain_NAPA	556.2189	556.2202	-1.4	[|LysoPE(18:1)|+2K-H]+
Brain_NAPA	558.2349	558.2359	-1.0	[|LysoPE(18:0)|+2K-H]+
Brain_NAPA	564.2489	564.2487	0.1	[|LysoPE(22:6)|+K]+
Brain_NAPA	568.2804	568.2800	0.4	[|LysoPE(22:4)|+K]+
Brain_NAPA	578.2046	578.2046	0.0	[|LysoPE(20:4)|+2K-H]+
Brain_NAPA	584.2528	584.2515	1.2	[|LysoPE(20:1)|+2K-H]+
Brain_NAPA	602.2048	602.2046	0.2	[|LysoPE(22:6)|+2K-H]+
Brain_NAPA	602.3609	602.3583	2.7	[|LysoPE(24:1)|+K]+
Brain_NAPA	604.5065	604.5066	-0.1	[|Cer(36:1)|+K]+
Brain_NAPA	620.5963	620.5976	-1.4	[|Cer(d40:2)|+H]+
Brain_NAPA	637.2727	637.2750	-2.3	[|LysoPI(18:1)|+K]+

Sample	Meas. *m/z*	Calc. *m/z*	Δm (mDa)	Tentative identification
Brain_NAPA	646.6124	646.6109	1.5	[|Cer(d40:0)|+Na]+
Brain_NAPA	648.6283	648.6289	-0.6	[|Cer(d42:2)|+H]+
Brain_NAPA	670.6100	670.6109	-0.9	[|Cer(d42:2)|+Na]+
Brain_NAPA	682.4572	682.4572	-0.1	[|CerP(d36:2)|+K]+
Brain_NAPA	683.5005	683.5011	-0.6	[|DG(38:4)|+K]+
Brain_NAPA	691.5261	691.5248	1.3	[|DG(38:3)|+2Na-H]+
Brain_NAPA	697.4768	697.4779	-1.1	[|PA(34:1)|+Na]+
Brain_NAPA	709.4192	709.4205	-1.4	[|PA(34:3)|+K]+
Brain_NAPA	709.5140	709.5168	-2.7	[|DG(40:5)|+K]+
Brain_NAPA	710.3581	710.3560	2.1	[|PE(28:1)|+2K-H]+
Brain_NAPA	713.4518	713.4518	0.0	[|PA(34:1)|+K]+
Brain_NAPA	721.4751	721.4779	-2.8	[|PA(36:3)|+Na]+
Brain_NAPA	721.4751	721.4755	-0.4	[|PA(34:0)|+2Na-H]+
Brain_NAPA	723.4925	723.4935	-1.1	[|PA(36:2)|+Na]+
Brain_NAPA	723.4925	723.4959	-3.5	[|PA(38:5)|+H]+
Brain_NAPA	725.3930	725.3921	0.9	[|PA(32:0)|+2K-H]+
Brain_NAPA	729.4823	729.4855	-3.2	[|DG(42:9)|+K]+
Brain_NAPA	730.4800	730.4784	1.6	[|PE(32:0)|+K]+
Brain_NAPA	735.4341	735.4362	-2.1	[|PA(36:4)|+K]+
Brain_NAPA	737.4528	737.4518	1.0	[|PA(36:3)|+K]+
Brain_NAPA	739.4093	739.4101	-0.7	[|DG(40:9)|+2K-H]+
Brain_NAPA	739.4671	739.4675	-0.4	[|PA(36:2)|+K]+
Brain_NAPA	741.4855	741.4831	2.4	[|PA(36:1)|+K]+
Brain_NAPA	743.4858	743.4834	2.5	[|PG(32:1)|+Na]+
Brain_NAPA	747.3769	747.3764	0.5	[|PA(34:3)|+2K-H]+
Brain_NAPA	747.4727	747.4727	0.0	[|DG(40:5)|+2K-H]+
Brain_NAPA	748.4504	748.4527	-2.3	[|HexCer(d32:1)|+2K-H]+
Brain_NAPA	748.5843	748.5851	-0.8	[|PE(36:0)|+H]+
Brain_NAPA	749.5055	749.5036	1.9	[|CE(20:4)|+2K-H]+
Brain_NAPA	749.5055	749.5068	-1.3	[|PA(36:0)|+2Na-H]+
Brain_NAPA	749.5055	749.5092	-3.7	[|PA(38:3)|+Na]+
Brain_NAPA	750.4496	750.4471	2.5	[|PE(34:4)|+K]+
Brain_NAPA	750.5424	750.5408	1.6	[|PE 36:2p|+Na]+
Brain_NAPA	750.5424	750.5432	-0.8	[|PE 38:5p|+H]+
Brain_NAPA	750.5846	750.5854	-0.8	[|HexCer(d36:1)|+Na]+
Brain_NAPA	751.4079	751.4077	0.2	[|PA(34:1)|+2K-H]+
Brain_NAPA	751.5221	751.5248	-2.7	[|PA(38:2)|+Na]+
Brain_NAPA	751.5221	751.5192	2.9	[|CE(20:3)|+2K-H]+
Brain_NAPA	753.5875	753.5905	-3.1	[|SM(d38:4)|+H]+
Brain_NAPA	753.5875	753.5881	-0.6	[|SM(d36:1)|+Na]+
Brain_NAPA	756.4937	756.4940	-0.3	[|PE(34:1)|+K]+
Brain_NAPA	756.5509	756.5538	-2.9	[|PC(34:3)|+H]+

Sample	Meas. *m/z*	Calc. *m/z*	Δm (mDa)	Tentative identification
Brain_NAPA	757.4192	757.4205	-1.3	[|PA(38:7)|+K]+
Brain_NAPA	758.5103	758.5097	0.6	[|PE(34:0)|+K]+
Brain_NAPA	759.4360	759.4362	-0.1	[|PA(38:6)|+K]+
Brain_NAPA	760.5851	760.5851	0.0	[|PC(34:1)|+H]+
Brain_NAPA	761.4511	761.4518	-0.7	[|PA(38:5)|+K]+
Brain_NAPA	763.4664	763.4675	-1.1	[|PA(38:4)|+K]+
Brain_NAPA	764.4027	764.4030	-0.3	[|PE(32:2)|+2K-H]+
Brain_NAPA	764.5422	764.5437	-1.5	[|HexCer(d36:2)|+K]+
Brain_NAPA	765.4846	765.4831	1.5	[|PA(38:3)|+K]+
Brain_NAPA	766.5136	766.5148	-1.2	[|PE 36:2p|+K]+
Brain_NAPA	766.5589	766.5594	-0.4	[|HexCer(d36:1)|+K]+
Brain_NAPA	767.4430	767.4414	1.6	[|DG(42:9)|+2K-H]+
Brain_NAPA	767.4979	767.4988	-0.9	[|PA(38:2)|+K]+
Brain_NAPA	768.4367	768.4343	2.4	[|PE(32:0)|+2K-H]+
Brain_NAPA	768.5281	768.5304	-2.3	[|PE 36:1p|+K]+
Brain_NAPA	769.4734	769.4755	-2.1	[|PA(38:4)|+2Na-H]+
Brain_NAPA	770.5077	770.5097	-2.0	[|PC(32:1)|+K]+
Brain_NAPA	770.5077	770.5095	-1.8	[|PE 38:6p|+Na]+
Brain_NAPA	770.5077	770.5071	0.6	[|PE 36:3p|+2Na-H]+
Brain_NAPA	770.5636	770.5670	-3.4	[|PE(36:0)|+Na]+
Brain_NAPA	772.5248	772.5228	2.0	[|PE 36:2p|+2Na-H]+
Brain_NAPA	772.5248	772.5252	-0.4	[|PE 38:5p|+Na]+
Brain_NAPA	773.3925	773.3921	0.4	[|PA(36:4)|+2K-H]+
Brain_NAPA	774.6009	774.6007	0.1	[|PE(38:1)|+H]+
Brain_NAPA	775.4087	775.4077	1.0	[|PA(36:3)|+2K-H]+
Brain_NAPA	777.4230	777.4234	-0.4	[|PA(36:2)|+2K-H]+
Brain_NAPA	778.4527	778.4550	-2.2	[|PE 34:1p|+2K-H]+
Brain_NAPA	778.6163	778.6167	-0.5	[|HexCer(d38:1)|+Na]+
Brain_NAPA	779.4389	779.4390	-0.1	[|PA(36:1)|+2K-H]+
Brain_NAPA	779.5547	779.5561	-1.4	[|PA(40:2)|+Na]+
Brain_NAPA	780.4932	780.4940	-0.9	[|PE(36:3)|+K]+
Brain_NAPA	780.5373	780.5386	-1.3	[|HexCer(d36:2(2OH))|+K]+
Brain_NAPA	782.5101	782.5097	0.4	[|PE(36:2)|+K]+
Brain_NAPA	782.5552	782.5543	0.9	[|HexCer(d36:1(2OH))|+K]+
Brain_NAPA	783.4334	783.4362	-2.8	[|PA(40:8)|+K]+
Brain_NAPA	784.5267	784.5253	1.3	[|PE(36:1)|+K]+
Brain_NAPA	785.4508	785.4518	-1.0	[|PA(40:7)|+K]+
Brain_NAPA	786.3900	786.3873	2.7	[|PE(34:5)|+2K-H]+
Brain_NAPA	786.4815	786.4835	-1.9	[|PE 38:6p|+K]+
Brain_NAPA	787.4666	787.4675	-0.9	[|PA(40:6)|+K]+
Brain_NAPA	788.4952	788.4991	-3.9	[|PE 38:5p|+K]+
Brain_NAPA	790.5137	790.5148	-1.0	[|PE 38:4p|+K]+

Sample	Meas. *m/z*	Calc. *m/z*	Δm (mDa)	Tentative identification
Brain_NAPA	792.4784	792.4789	-0.5	[|HexCer(d34:1(2OH))|+2K-H]+
Brain_NAPA	792.5282	792.5304	-2.2	[|PE 38:3p|+K]+
Brain_NAPA	793.4956	793.4966	-1.0	[|PG(34:1)|+2Na-H]+
Brain_NAPA	793.4956	793.4990	-3.4	[|PG(36:4)|+Na]+
Brain_NAPA	794.4506	794.4499	0.7	[|PE(34:1)|+2K-H]+
Brain_NAPA	794.5454	794.5461	-0.7	[|PE 38:2p|+K]+
Brain_NAPA	794.6118	794.6117	0.2	[|HexCer(d38:1(2OH))|+Na]+
Brain_NAPA	795.3759	795.3764	-0.5	[|PA(38:7)|+2K-H]+
Brain_NAPA	796.4673	796.4656	1.7	[|PE(34:0)|+2K-H]+
Brain_NAPA	796.5259	796.5228	3.1	[|PE 38:4p|+2Na-H]+
Brain_NAPA	796.5259	796.5253	0.6	[|PC(34:2)|+K]+
Brain_NAPA	797.3927	797.3921	0.7	[|PA(38:6)|+2K-H]+
Brain_NAPA	798.4667	798.4682	-1.5	[|PS(34:2)|+K]+
Brain_NAPA	798.5404	798.5408	-0.4	[|PE 40:6p|+Na]+
Brain_NAPA	798.5404	798.5410	-0.6	[|PC(34:1)|+K]+
Brain_NAPA	798.5404	798.5384	2.0	[|PE 38:3p|+2Na-H]+
Brain_NAPA	799.4082	799.4077	0.5	[|PA(38:5)|+2K-H]+
Brain_NAPA	800.5572	800.5565	0.7	[|PE 40:5p|+Na]+
Brain_NAPA	800.5572	800.5541	3.1	[|PE 38:2p|+2Na-H]+
Brain_NAPA	800.5572	800.5566	0.6	[|PC(34:0)|+K]+
Brain_NAPA	800.5572	800.5589	-1.7	[|PE 42:8p|+H]+
Brain_NAPA	801.4225	801.4234	-0.9	[|PA(38:4)|+2K-H]+
Brain_NAPA	801.5635	801.5640	-0.5	[|PG(38:3)|+H]+
Brain_NAPA	801.5635	801.5616	1.9	[|PG(36:0)|+Na]+
Brain_NAPA	802.4783	802.4784	-0.1	[|PE(38:6)|+K]+
Brain_NAPA	804.4695	804.4706	-1.1	[|PE 36:2p|+2K-H]+
Brain_NAPA	804.5498	804.5490	0.9	[|PC(34:1)|+2Na-H]+
Brain_NAPA	804.5498	804.5514	-1.5	[|PC(36:4)|+Na]+
Brain_NAPA	804.5498	804.5538	-3.9	[|PC(38:7)|+H]+
Brain_NAPA	804.6327	804.6324	0.3	[|HexCer(d40:2)|+Na]+
Brain_NAPA	806.5084	806.5097	-1.3	[|PE(38:4)|+K]+
Brain_NAPA	806.6471	806.6480	-0.9	[|HexCer(d42:1)|+Na]+
Brain_NAPA	808.4634	808.4656	-2.2	[|PC(32:1)|+2K-H]+
Brain_NAPA	808.5692	808.5699	-0.8	[|HexCer(d38:2(2OH))|+K]+
Brain_NAPA	808.6304	808.6273	3.1	[|HexCer(d39:1(2OH))|+Na]+
Brain_NAPA	810.5436	810.5410	2.6	[|PE(38:2)|+K]+
Brain_NAPA	810.5841	810.5856	-1.5	[|HexCer(d38:1(2OH))|+K]+
Brain_NAPA	811.4862	811.4886	-2.4	[|PG(36:3)|+K]+
Brain_NAPA	813.5036	813.5043	-0.6	[|PG(36:2)|+K]+
Brain_NAPA	814.5135	814.5148	-1.2	[|PE 40:6p|+K]+
Brain_NAPA	816.4337	816.4343	-0.6	[|PE(36:4)|+2K-H]+
Brain_NAPA	816.5286	816.5304	-1.8	[|PE 40:5p|+K]+

Sample	Meas. *m/z*	Calc. *m/z*	Δm (mDa)	Tentative identification
Brain_NAPA	818.5454	818.5461	-0.6	[|PE 40:4p|+K]+
Brain_NAPA	818.6482	818.6480	0.2	[|HexCer(d41:2)|+Na]+
Brain_NAPA	820.4654	820.4656	-0.1	[|PE(36:2)|+2K-H]+
Brain_NAPA	820.5258	820.5228	3.0	[|PE 40:6p|+2Na-H]+
Brain_NAPA	820.5258	820.5253	0.5	[|PC(36:4)|+K]+
Brain_NAPA	820.6037	820.6063	-2.7	[|HexCer(d42:2)|+K]+
Brain_NAPA	820.6037	820.6062	-2.6	[|PS(38:0)|+H]+
Brain_NAPA	821.3937	821.3921	1.6	[|PA(40:8)|+2K-H]+
Brain_NAPA	822.4820	822.4812	0.8	[|PE(36:1)|+2K-H]+
Brain_NAPA	822.6444	822.6430	1.4	[|HexCer(t40:1)|+Na]+
Brain_NAPA	823.4074	823.4077	-0.3	[|PA(40:7)|+2K-H]+
Brain_NAPA	824.4367	824.4393	-2.7	[|PE 38:6p|+2K-H]+
Brain_NAPA	824.5559	824.5541	1.9	[|PE 40:4p|+2Na-H]+
Brain_NAPA	824.5559	824.5566	-0.7	[|PC(36:2)|+K]+
Brain_NAPA	824.5559	824.5565	-0.5	[|PE 42:7p|+Na]+
Brain_NAPA	824.6006	824.6012	-0.6	[|HexCer(d39:1(2OH))|+K]+
Brain_NAPA	825.4212	825.4234	-2.1	[|PA(40:6)|+2K-H]+
Brain_NAPA	826.5724	826.5721	0.3	[|PE 42:6p|+Na]+
Brain_NAPA	826.5724	826.5697	2.7	[|PE 40:3p|+2Na-H]+
Brain_NAPA	826.5724	826.5723	0.1	[|PC(36:1)|+K]+
Brain_NAPA	827.4574	827.4601	-2.8	[|PG(34:0)|+2K-H]+
Brain_NAPA	828.4933	828.4973	-4.0	[|PI-Cer(t33:0)|+2Na-H]+
Brain_NAPA	828.4933	828.4940	-0.7	[|PE(40:7)|+K]+
Brain_NAPA	830.5097	830.5097	0.1	[|PE(40:6)|+K]+
Brain_NAPA	830.6495	830.6456	3.9	[|HexCer(d40:0)|+2Na-H]+
Brain_NAPA	831.4342	831.4362	-1.9	[|PA(44:12)|+K]+
Brain_NAPA	832.5020	832.5019	0.1	[|PE 38:2p|+2K-H]+
Brain_NAPA	832.5841	832.5851	-1.0	[|PC(40:7)|+H]+
Brain_NAPA	832.5841	832.5827	1.4	[|PC(38:4)|+Na]+
Brain_NAPA	832.5841	832.5803	3.8	[|PC(36:1)|+2Na-H]+
Brain_NAPA	832.6634	832.6637	-0.3	[|HexCer(d42:2)|+Na]+
Brain_NAPA	834.6184	834.6220	-3.6	[|HexCer(d41:2)|+K]+
Brain_NAPA	834.6752	834.6793	-4.2	[|HexCer(d42:1)|+Na]+
Brain_NAPA	836.4942	836.4969	-2.6	[|PC(34:1)|+2K-H]+
Brain_NAPA	836.6038	836.6012	2.5	[|HexCer(d42:2(2OH))|+K]+
Brain_NAPA	838.4414	838.4397	1.6	[|PS(34:1)|+2K-H]+
Brain_NAPA	838.5127	838.5148	-2.0	[|PE 42:8p|+K]+
Brain_NAPA	838.5127	838.5125	0.2	[|PC(34:0)|+2K-H]+
Brain_NAPA	838.6164	838.6168	-0.4	[|PI-Cer(38:0)|+H]+
Brain_NAPA	838.6164	838.6169	-0.5	[|HexCer(t40:1)|+K]+
Brain_NAPA	840.4340	840.4343	-0.3	[|PE(38:6)|+2K-H]+
Brain_NAPA	840.5281	840.5304	-2.3	[|PE 42:7p|+K]+

Sample	Meas. *m/z*	Calc. *m/z*	Δm (mDa)	Tentative identification
Brain_NAPA	842.4518	842.4499	1.9	[|PE(38:5)|+2K-H]+
Brain_NAPA	844.4653	844.4656	-0.2	[|PE(38:4)|+2K-H]+
Brain_NAPA	844.5264	844.5253	1.0	[|PC(38:6)|+K]+
Brain_NAPA	844.5264	844.5228	3.6	[|PE 42:8p|+2Na-H]+
Brain_NAPA	846.4656	846.4682	-2.6	[|PS(38:6)|+K]+
Brain_NAPA	846.5421	846.5410	1.2	[|PC(38:5)|+K]+
Brain_NAPA	846.5421	846.5384	3.7	[|PE 42:7p|+2Na-H]+
Brain_NAPA	848.4970	848.4929	4.1	[|Sulfatide(d36:3)|+2Na-H]+
Brain_NAPA	848.4970	848.4969	0.1	[|PE(38:2)|+2K-H]+
Brain_NAPA	848.5585	848.5566	1.9	[|PC(38:4)|+K]+
Brain_NAPA	848.6348	848.6376	-2.8	[|HexCer(d42:2)|+K]+
Brain_NAPA	850.5109	850.5125	-1.6	[|PE(38:1)|+2K-H]+
Brain_NAPA	850.5109	850.5086	2.4	[|Sulfatide(d36:2)|+2Na-H]+
Brain_NAPA	851.4586	851.4601	-1.6	[|PG(36:2)|+2K-H]+
Brain_NAPA	854.4858	854.4863	-0.5	[|PE 40:5p|+2K-H]+
Brain_NAPA	855.6332	855.6351	-1.9	[|SM(d44:6)|+Na]+
Brain_NAPA	856.4983	856.5019	-3.6	[|PE 40:4p|+2K-H]+
Brain_NAPA	856.5822	856.5803	1.9	[|PC(38:3)|+2Na-H]+
Brain_NAPA	856.5822	856.5827	-0.5	[|PC(40:6)|+Na]+
Brain_NAPA	858.4826	858.4812	1.4	[|PC(36:4)|+2K-H]+
Brain_NAPA	860.6913	860.6950	-3.7	[|HexCer(d44:2)|+Na]+
Brain_NAPA	861.5325	861.5366	-4.1	[|LysylPG(30:0)|+K]+
Brain_NAPA	862.4423	862.4397	2.5	[|PS(36:3)|+2K-H]+
Brain_NAPA	862.5310	862.5333	-2.3	[|PE(42:7)|+2Na-H]+
Brain_NAPA	862.6244	862.6272	-2.8	[|PC(38:0)|+2Na-H]+
Brain_NAPA	862.6244	862.6250	-0.6	[|LacCer (d34:1)|+H]+
Brain_NAPA	864.4545	864.4554	-0.9	[|PS(36:2)|+2K-H]+
Brain_NAPA	864.6310	864.6325	-1.6	[|HexCer(d42:2(2OH))|+K]+
Brain_NAPA	866.4477	866.4499	-2.2	[|PE(40:7)|+2K-H]+
Brain_NAPA	866.6459	866.6481	-2.2	[|PI-Cer(40:0)|+H]+
Brain_NAPA	866.6459	866.6482	-2.3	[|HexCer(d42:1(2OH))|+K]+
Brain_NAPA	868.4639	868.4656	-1.6	[|PE(40:6)|+2K-H]+
Brain_NAPA	869.3926	869.3921	0.5	[|PA(44:12)|+2K-H]+
Brain_NAPA	870.5392	870.5410	-1.7	[|PC(40:7)|+K]+
Brain_NAPA	872.4969	872.4969	0.1	[|PE(40:4)|+2K-H]+
Brain_NAPA	872.5561	872.5566	-0.6	[|PC(40:6)|+K]+
Brain_NAPA	874.5007	874.4995	1.2	[|PS(40:6)|+K]+
Brain_NAPA	874.5900	874.5935	-3.5	[|HexCer(d41:1)|+2K-H]+
Brain_NAPA	876.6462	876.6429	3.3	[|PE(42:0)|+2Na-H]+
Brain_NAPA	878.6463	878.6482	-1.9	[|HexCer(d43:2(2OH))|+K]+
Brain_NAPA	880.4696	880.4656	4.1	[|PC(38:7)|+2K-H]+
Brain_NAPA	881.4691	881.4730	-3.9	[|PG(42:10)|+K]+

Sample	Meas. *m/z*	Calc. *m/z*	Δm (mDa)	Tentative identification
Brain_NAPA	884.4695	884.4721	-2.6	[|Sulfatide(d36:1)|+2K-H]+
Brain_NAPA	885.4677	885.4653	2.4	[|PG(42:11)|+2Na-H]+
Brain_NAPA	888.4513	888.4554	-4.1	[|PS(38:4)|+2K-H]+
Brain_NAPA	890.5924	890.5906	1.9	[|PS(44:7)|+H]+
Brain_NAPA	892.4661	892.4656	0.5	[|PE(42:8)|+2K-H]+
Brain_NAPA	894.4799	894.4812	-1.3	[|PE(42:7)|+2K-H]+
Brain_NAPA	901.4778	901.4758	2.1	[|PG(40:5)|+2K-H]+
Brain_NAPA	904.6056	904.6041	1.5	[|HexCer(d42:1(2OH))|+2K-H]+
Brain_NAPA	904.6056	904.6040	1.6	[|PI-Cer(40:0)|+K]+
Brain_NAPA	906.5692	906.5712	-2.0	[|Sulfatide(d40:2)|+2Na-H]+
Brain_NAPA	911.4453	911.4449	0.4	[|PI(34:2)|+2K-H]+
Brain_NAPA	912.4571	912.4554	1.7	[|PS(40:6)|+2K-H]+
Brain_NAPA	916.6075	916.6041	3.4	[|HexCer(d43:2(2OH))|+2K-H]+
Brain_NAPA	923.5045	923.5046	-0.2	[|PI(38:5)|+K]+
Brain_NAPA	925.5208	925.5203	0.5	[|PI(38:4)|+K]+
Brain_NAPA	930.6127	930.6101	2.6	[|Sulfatide(d42:1)|+K]+
Brain_NAPA	934.5997	934.6025	-2.8	[|Sulfatide(d42:2)|+2Na-H]+
Brain_NAPA	935.4418	935.4449	-3.0	[|PI(36:4)|+2K-H]+
Brain_NAPA	938.5145	938.5190	-4.5	[|Sulfatide(d40:2)|+2K-H]+
Brain_NAPA	943.4270	943.4288	-1.9	[|PG(44:12)|+2K-H]+
Brain_NAPA	959.4470	959.4449	2.2	[|PI(38:6)|+2K-H]+
Brain_NAPA	960.5284	960.5282	0.2	[|PC(44:9)|+2K-H]+
Brain_NAPA	961.4617	961.4605	1.2	[|PI(38:5)|+2K-H]+
Brain_NAPA	963.4755	963.4762	-0.6	[|PI(38:4)|+2K-H]+
Brain_NAPA	964.5310	964.5347	-3.7	[|Sulfatide(d42:3)|+2K-H]+
Brain_NAPA	966.5485	966.5503	-1.9	[|Sulfatide(d42:2)|+2K-H]+
Brain_NAPA	987.4742	987.4762	-1.9	[|PI(40:6)|+2K-H]+
Brain_NAPA	1047.6245	1047.6241	0.4	[|TG(62:16)|+2K-H]+

Table S2. Tentative lipid identifications based on mass accuracy tolerance of Δ*m/z* ≤ ±5 mDa from analysis of mouse lung tissue sections by MALDI- and NAPA-LDI-MSI. For *m/z* values with multiple potential interpretations, all possibilities are listed.

Sample	Meas. *m/z*	Calc. *m/z*	Δm (mDa)	Tentative identification
Lung_MALDI	327.2271	327.2271	0.0	[|FA(18:1)|+2Na-H]+
Lung_MALDI	329.2428	329.2427	0.1	[|FA(18:0)|+2Na-H]+
Lung_MALDI	333.1592	333.1593	0.0	[|FA(16:0)|+2K-H]+
Lung_MALDI	369.3515	369.3516	-0.1	[|Cholesterol (-H2O)|+H]+
Lung_MALDI	479.0949	479.0938	1.0	[|FMN|+Na]+
Lung_MALDI	496.3386	496.3398	-1.2	[|LysoPC(16:0)|+H]+
Lung_MALDI	498.2554	498.2567	-1.3	[|LysoPE(16:0)|+2Na-H]+
Lung_MALDI	518.3202	518.3217	-1.6	[|LysoPC(16:0)|+Na]+
Lung_MALDI	524.3697	524.3711	-1.3	[|LysoPC(18:0)|+H]+
Lung_MALDI	526.2865	526.2880	-1.6	[|LysoPE(18:0)|+2Na-H]+
Lung_MALDI	534.2966	534.2957	1.0	[|LysoPC(16:0)|+K]+
Lung_MALDI	546.3517	546.3530	-1.3	[|LysoPC(18:0)|+Na]+
Lung_MALDI	554.2668	554.2644	2.5	[|LysoPC(18:4)|+K]+
Lung_MALDI	558.2982	558.2957	2.6	[|LysoPC(18:2)|+K]+
Lung_MALDI	558.4836	558.4857	-2.1	[|Cer(d34:2)|+Na]+
Lung_MALDI	560.5007	560.5013	-0.6	[|Cer(d34:1)|+Na]+
Lung_MALDI	561.2013	561.1992	2.1	[|LysoPG(16:0)|+2K-H]+
Lung_MALDI	562.3274	562.3270	0.4	[|LysoPC(18:0)|+K]+
Lung_MALDI	568.2817	568.2800	1.7	[|LysoPE(22:4)|+K]+
Lung_MALDI	592.2817	592.2800	1.7	[|LysoPE(24:6)|+K]+
Lung_MALDI	610.3281	610.3270	1.1	[|LysoPC(22:4)|+K]+
Lung_MALDI	615.4958	615.4959	-0.1	[|DG(34:2)|+Na]+
Lung_MALDI	617.5117	617.5140	-2.2	[|DG(36:4)|+H]+
Lung_MALDI	617.5117	617.5116	0.2	[|DG(34:1)|+Na]+
Lung_MALDI	618.3900	618.3896	0.5	[|LysoPC(22:0)|+K]+
Lung_MALDI	637.4790	637.4778	1.2	[|DG(34:2)|+2Na-H]+
Lung_MALDI	639.4951	639.4935	1.6	[|DG(34:1)|+2Na-H]+
Lung_MALDI	639.4951	639.4959	-0.8	[|DG(36:4)|+Na]+
Lung_MALDI	641.5108	641.5140	-3.1	[|DG(38:6)|+H]+
Lung_MALDI	641.5108	641.5116	-0.7	[|DG(36:3)|+Na]+
Lung_MALDI	643.5266	643.5272	-0.6	[|DG(36:2)|+Na]+
Lung_MALDI	643.5266	643.5296	-3.0	[|DG(38:5)|+H]+
Lung_MALDI	656.4245	656.4262	-1.6	[|PE(28:1)|+Na]+
Lung_MALDI	661.4784	661.4778	0.6	[|DG(36:4)|+2Na-H]+
Lung_MALDI	662.4488	662.4496	-0.8	[|CerP(d34:1)|+2Na-H]+
Lung_MALDI	663.4950	663.4935	1.6	[|DG(36:3)|+2Na-H]+
Lung_MALDI	663.4950	663.4959	-0.9	[|DG(38:6)|+Na]+
Lung_MALDI	663.4950	663.4983	-3.3	[|DG(40:9)|+H]+
Lung_MALDI	665.5093	665.5116	-2.2	[|DG(38:5)|+Na]+
Lung_MALDI	665.5093	665.5091	0.2	[|DG(36:2)|+2Na-H]+
Lung_MALDI	666.4819	666.4833	-1.4	[|CerP(d36:2)|+Na]+
Lung_MALDI	666.5756	666.5772	-1.6	[|Cer(d40:1)|+2Na-H]+
Lung_MALDI	668.5906	668.5928	-2.2	[|Cer(d40:0)|+2Na-H]+

Sample	Meas. *m/z*	Calc. *m/z*	Δm (mDa)	Tentative identification
Lung_MALDI	669.4471	669.4490	-1.9	[|PA(34:4)|+H]+
Lung_MALDI	669.4471	669.4466	0.5	[|PA(32:1)|+Na]+
Lung_MALDI	670.6092	670.6109	-1.7	[|Cer(d42:2)|+Na]+
Lung_MALDI	672.4557	672.4575	-1.8	[|PC(26:0)|+Na]+
Lung_MALDI	682.4568	682.4572	-0.5	[|CerP(d36:2)|+K]+
Lung_MALDI	685.4190	685.4205	-1.6	[|PA(32:1)|+K]+
Lung_MALDI	688.4638	688.4652	-1.4	[|CerP(d36:2)|+2Na-H]+
Lung_MALDI	689.5095	689.5091	0.3	[|DG(38:4)|+2Na-H]+
Lung_MALDI	691.4286	691.4309	-2.3	[|PA(34:4)|+Na]+
Lung_MALDI	691.4286	691.4285	0.1	[|PA(32:1)|+2Na-H]+
Lung_MALDI	693.4441	693.4466	-2.5	[|PA(34:3)|+Na]+
Lung_MALDI	693.4441	693.4442	0.0	[|PA(32:0)|+2Na-H]+
Lung_MALDI	695.4613	695.4646	-3.4	[|PA(36:5)|+H]+
Lung_MALDI	697.4765	697.4779	-1.4	[|PA(34:1)|+Na]+
Lung_MALDI	707.4587	707.4622	-3.5	[|DG(40:9)|+2Na-H]+
Lung_MALDI	709.4184	709.4205	-2.1	[|PA(34:3)|+K]+
Lung_MALDI	709.5132	709.5168	-3.5	[|DG(40:5)|+K]+
Lung_MALDI	713.4505	713.4518	-1.3	[|PA(34:1)|+K]+
Lung_MALDI	717.4431	717.4466	-3.4	[|PA(36:5)|+Na]+
Lung_MALDI	719.4585	719.4598	-1.3	[|PA(34:1)|+2Na-H]+
Lung_MALDI	720.4127	720.4131	-0.5	[|CerP(d36:2)|+2K-H]+
Lung_MALDI	721.3582	721.3608	-2.5	[|PA(32:2)|+2K-H]+
Lung_MALDI	721.4763	721.4755	0.8	[|PA(34:0)|+2Na-H]+
Lung_MALDI	721.4763	721.4779	-1.6	[|PA(36:3)|+Na]+
Lung_MALDI	723.4923	723.4935	-1.2	[|PA(36:2)|+Na]+
Lung_MALDI	725.3922	725.3921	0.1	[|PA(32:0)|+2K-H]+
Lung_MALDI	725.5552	725.5568	-1.6	[|SM(d34:1)|+Na]+
Lung_MALDI	726.5094	726.5068	2.5	[|PC(32:4)|+H]+
Lung_MALDI	728.5183	728.5201	-1.8	[|PC(30:0)|+Na]+
Lung_MALDI	729.4821	729.4855	-3.4	[|DG(42:9)|+K]+
Lung_MALDI	731.4014	731.4049	-3.5	[|PA(36:6)|+K]+
Lung_MALDI	732.5516	732.5538	-2.2	[|PC(32:1)|+H]+
Lung_MALDI	733.4176	733.4205	-2.9	[|PA(36:5)|+K]+
Lung_MALDI	735.4333	735.4362	-2.9	[|PA(36:4)|+K]+
Lung_MALDI	737.4510	737.4518	-0.8	[|PA(36:3)|+K]+
Lung_MALDI	739.4661	739.4675	-1.3	[|PA(36:2)|+K]+
Lung_MALDI	741.4830	741.4831	-0.1	[|PA(36:1)|+K]+
Lung_MALDI	741.5293	741.5307	-1.5	[|SM(d34:1)|+K]+
Lung_MALDI	742.5334	742.5357	-2.3	[|PE(34:0)|+Na]+
Lung_MALDI	743.4594	743.4598	-0.5	[|PA(36:3)|+2Na-H]+
Lung_MALDI	743.4594	743.4622	-2.9	[|PA(38:6)|+Na]+
Lung_MALDI	744.4909	744.4915	-0.5	[|PE 34:2p|+2Na-H]+
Lung_MALDI	744.4909	744.4940	-3.1	[|PC(30:0)|+K]+
Lung_MALDI	745.4758	745.4755	0.3	[|PA(36:2)|+2Na-H]+
Lung_MALDI	745.4758	745.4779	-2.1	[|PA(38:5)|+Na]+
Lung_MALDI	746.5668	746.5694	-2.7	[|PE(36:1)|+H]+
Lung_MALDI	747.3748	747.3764	-1.6	[|PA(34:3)|+2K-H]+

Sample	Meas. *m/z*	Calc. *m/z*	Δm (mDa)	Tentative identification
Lung_MALDI	747.4912	747.4911	0.1	[|PA(36:1)|+2Na-H]+
Lung_MALDI	747.4912	747.4935	-2.3	[|PA(38:4)|+Na]+
Lung_MALDI	747.4912	747.4879	3.3	[|CE(20:5)|+2K-H]+
Lung_MALDI	748.5818	748.5851	-3.3	[|PE(36:0)|+H]+
Lung_MALDI	749.5095	749.5116	-2.1	[|PA(40:6)|+H]+
Lung_MALDI	749.5095	749.5092	0.3	[|PA(38:3)|+Na]+
Lung_MALDI	749.5095	749.5068	2.7	[|PA(36:0)|+2Na-H]+
Lung_MALDI	750.5753	750.5772	-1.9	[|CerP(d42:2)|+Na]+
Lung_MALDI	751.4070	751.4077	-0.7	[|PA(34:1)|+2K-H]+
Lung_MALDI	751.5240	751.5248	-0.8	[|PA(38:2)|+Na]+
Lung_MALDI	751.5240	751.5272	-3.2	[|PA(40:5)|+H]+
Lung_MALDI	753.5864	753.5881	-1.7	[|SM(d36:1)|+Na]+
Lung_MALDI	754.5339	754.5357	-1.8	[|PC(32:1)|+Na]+
Lung_MALDI	757.4175	757.4205	-3.0	[|PA(38:7)|+K]+
Lung_MALDI	758.5076	758.5097	-2.0	[|PE(34:0)|+K]+
Lung_MALDI	759.4335	759.4362	-2.7	[|PA(38:6)|+K]+
Lung_MALDI	760.5828	760.5851	-2.3	[|PC(34:1)|+H]+
Lung_MALDI	761.4494	761.4518	-2.4	[|PA(38:5)|+K]+
Lung_MALDI	763.4657	763.4675	-1.8	[|PA(38:4)|+K]+
Lung_MALDI	764.5151	764.5177	-2.5	[|PE(34:0)|+2Na-H]+
Lung_MALDI	765.4836	765.4831	0.4	[|PA(38:3)|+K]+
Lung_MALDI	766.5505	766.5511	-0.7	[|CerP(d42:2)|+K]+
Lung_MALDI	767.4593	767.4598	-0.5	[|PA(38:5)|+2Na-H]+
Lung_MALDI	767.4593	767.4622	-2.9	[|PA(40:8)|+Na]+
Lung_MALDI	767.4986	767.4988	-0.2	[|PA(38:2)|+K]+
Lung_MALDI	768.4904	768.4915	-1.1	[|PE 36:4p|+2Na-H]+
Lung_MALDI	768.4904	768.4940	-3.6	[|PC(32:2)|+K]+
Lung_MALDI	768.5510	768.5514	-0.4	[|PE(36:1)|+Na]+
Lung_MALDI	768.5510	768.5538	-2.8	[|PE(38:4)|+H]+
Lung_MALDI	769.4746	769.4755	-0.9	[|PA(38:4)|+2Na-H]+
Lung_MALDI	769.4746	769.4779	-3.3	[|PA(40:7)|+Na]+
Lung_MALDI	769.5604	769.5620	-1.6	[|SM(d36:1)|+K]+
Lung_MALDI	770.5046	770.5071	-2.5	[|PE 36:3p|+2Na-H]+
Lung_MALDI	770.5645	770.5670	-2.5	[|PE(36:0)|+Na]+
Lung_MALDI	771.3749	771.3764	-1.5	[|PA(36:5)|+2K-H]+
Lung_MALDI	772.5232	772.5252	-1.9	[|PE 38:5p|+Na]+
Lung_MALDI	772.5232	772.5228	0.5	[|PE 36:2p|+2Na-H]+
Lung_MALDI	773.3897	773.3921	-2.3	[|PA(36:4)|+2K-H]+
Lung_MALDI	774.5757	774.5748	0.9	[|CerP(d42:1)|+2Na-H]+
Lung_MALDI	775.4074	775.4077	-0.3	[|PA(36:3)|+2K-H]+
Lung_MALDI	775.5227	775.5248	-2.1	[|PA(40:4)|+Na]+
Lung_MALDI	775.5227	775.5224	0.3	[|PA(38:1)|+2Na-H]+
Lung_MALDI	775.5227	775.5192	3.5	[|CE(22:5)|+2K-H]+
Lung_MALDI	777.4222	777.4234	-1.1	[|PA(36:2)|+2K-H]+
Lung_MALDI	778.4751	778.4784	-3.3	[|PE(36:4)|+K]+
Lung_MALDI	778.5325	778.5357	-3.2	[|PC(34:3)|+Na]+
Lung_MALDI	779.4385	779.4390	-0.5	[|PA(36:1)|+2K-H]+

Sample	**Meas. *m/z***	**Calc. *m/z***	**Δm (mDa)**	**Tentative identification**
Lung_MALDI	780.4907	780.4940	-3.3	[|PE(36:3)|+K]+
Lung_MALDI	780.5492	780.5514	-2.2	[|PC(34:2)|+Na]+
Lung_MALDI	781.6173	781.6194	-2.1	[|SM(d38:1)|+Na]+
Lung_MALDI	782.5649	782.5670	-2.2	[|PC(34:1)|+Na]+
Lung_MALDI	783.4344	783.4362	-1.7	[|PA(40:8)|+K]+
Lung_MALDI	784.5800	784.5827	-2.7	[|PC(34:0)|+Na]+
Lung_MALDI	785.4481	785.4518	-3.7	[|PA(40:7)|+K]+
Lung_MALDI	787.4666	787.4675	-0.9	[|PA(40:6)|+K]+
Lung_MALDI	789.4814	789.4831	-1.8	[|PA(40:5)|+K]+
Lung_MALDI	792.4820	792.4789	3.1	[|HexCer(d34:1(2OH))|+2K-H]+
Lung_MALDI	793.4777	793.4755	2.2	[|PA(40:6)|+2Na-H]+
Lung_MALDI	793.4777	793.4803	-2.6	[|PA(44:12)|+H]+
Lung_MALDI	794.4499	794.4460	3.9	[|Sulfatide(d32:2)|+2Na-H]+
Lung_MALDI	794.4499	794.4499	0.0	[|PE(34:1)|+2K-H]+
Lung_MALDI	795.4878	795.4911	-3.4	[|PA(40:5)|+2Na-H]+
Lung_MALDI	796.4659	796.4656	0.3	[|PE(34:0)|+2K-H]+
Lung_MALDI	796.5221	796.5228	-0.6	[|PE 38:4p|+2Na-H]+
Lung_MALDI	796.5221	796.5253	-3.2	[|PC(34:2)|+K]+
Lung_MALDI	796.5798	796.5827	-2.9	[|PE(38:1)|+Na]+
Lung_MALDI	797.3945	797.3921	2.4	[|PA(38:6)|+2K-H]+
Lung_MALDI	797.5903	797.5933	-3.0	[|SM(d38:1)|+K]+
Lung_MALDI	798.5384	798.5410	-2.5	[|PC(34:1)|+K]+
Lung_MALDI	798.5384	798.5408	-2.4	[|PE 40:6p|+Na]+
Lung_MALDI	798.5384	798.5384	0.0	[|PE 38:3p|+2Na-H]+
Lung_MALDI	799.4075	799.4077	-0.2	[|PA(38:5)|+2K-H]+
Lung_MALDI	801.4200	801.4234	-3.3	[|PA(38:4)|+2K-H]+
Lung_MALDI	801.5408	801.5381	2.7	[|PA(40:2)|+2Na-H]+
Lung_MALDI	804.5490	804.5490	0.1	[|PC(34:1)|+2Na-H]+
Lung_MALDI	804.5490	804.5514	-2.3	[|PC(36:4)|+Na]+
Lung_MALDI	806.5067	806.5097	-2.9	[|PE(38:4)|+K]+
Lung_MALDI	806.5653	806.5646	0.6	[|PC(34:0)|+2Na-H]+
Lung_MALDI	806.5653	806.5670	-1.8	[|PC(36:3)|+Na]+
Lung_MALDI	807.6322	807.6351	-2.8	[|SM(d40:2)|+Na]+
Lung_MALDI	808.5808	808.5827	-1.9	[|PC(36:2)|+Na]+
Lung_MALDI	809.6489	809.6507	-1.8	[|SM(d40:1)|+Na]+
Lung_MALDI	810.5975	810.6007	-3.3	[|PC(38:4)|+H]+
Lung_MALDI	810.5975	810.5983	-0.9	[|PC(36:1)|+Na]+
Lung_MALDI	812.5159	812.5177	-1.8	[|PE(38:4)|+2Na-H]+
Lung_MALDI	815.4611	815.4622	-1.1	[|PA(44:12)|+Na]+
Lung_MALDI	816.5450	816.5490	-4.0	[|PE(38:2)|+2Na-H]+
Lung_MALDI	818.5608	818.5646	-3.8	[|PE(38:1)|+2Na-H]+
Lung_MALDI	820.4636	820.4656	-1.9	[|PE(36:2)|+2K-H]+
Lung_MALDI	820.5229	820.5228	0.1	[|PE 40:6p|+2Na-H]+
Lung_MALDI	820.5229	820.5253	-2.5	[|PC(36:4)|+K]+
Lung_MALDI	822.4790	822.4773	1.7	[|Sulfatide(d34:2)|+2Na-H]+
Lung_MALDI	822.4790	822.4812	-2.2	[|PE(36:1)|+2K-H]+
Lung_MALDI	822.5377	822.5408	-3.2	[|PE 42:8p|+Na]+

Sample	Meas. *m/z*	Calc. *m/z*	Δm (mDa)	Tentative identification
Lung_MALDI	822.5377	822.5384	-0.8	[|PE 40:5p|+2Na-H]+
Lung_MALDI	822.5377	822.5410	-3.3	[|PC(36:3)|+K]+
Lung_MALDI	824.5543	824.5541	0.3	[|PE 40:4p|+2Na-H]+
Lung_MALDI	824.5543	824.5566	-2.3	[|PC(36:2)|+K]+
Lung_MALDI	824.5543	824.5565	-2.1	[|PE 42:7p|+Na]+
Lung_MALDI	824.6116	824.6140	-2.3	[|PE(40:1)|+Na]+
Lung_MALDI	825.6215	825.6246	-3.1	[|SM(d40:1)|+K]+
Lung_MALDI	826.4586	826.4550	3.6	[|PE 38:5p|+2K-H]+
Lung_MALDI	826.5707	826.5697	1.0	[|PE 40:3p|+2Na-H]+
Lung_MALDI	826.5707	826.5723	-1.6	[|PC(36:1)|+K]+
Lung_MALDI	826.5707	826.5721	-1.4	[|PE 42:6p|+Na]+
Lung_MALDI	827.4368	827.4390	-2.2	[|PA(40:5)|+2K-H]+
Lung_MALDI	827.7080	827.7099	-1.9	[|TG(48:1)|+Na]+
Lung_MALDI	828.4903	828.4940	-3.7	[|PE(40:7)|+K]+
Lung_MALDI	828.5496	828.5490	0.7	[|PC(36:3)|+2Na-H]+
Lung_MALDI	828.5496	828.5514	-1.7	[|PC(38:6)|+Na]+
Lung_MALDI	829.7236	829.7256	-1.9	[|TG(48:0)|+Na]+
Lung_MALDI	830.5647	830.5646	0.1	[|PC(36:2)|+2Na-H]+
Lung_MALDI	830.5647	830.5670	-2.3	[|PC(38:5)|+Na]+
Lung_MALDI	832.5813	832.5827	-1.4	[|PC(38:4)|+Na]+
Lung_MALDI	832.5813	832.5803	1.0	[|PC(36:1)|+2Na-H]+
Lung_MALDI	832.5813	832.5851	-3.8	[|PC(40:7)|+H]+
Lung_MALDI	833.6478	833.6483	-0.5	[|SM(d40:0)|+2Na-H]+
Lung_MALDI	834.5192	834.5232	-3.9	[|PS(36:1)|+2Na-H]+
Lung_MALDI	835.6642	835.6664	-2.1	[|SM(d42:2)|+Na]+
Lung_MALDI	836.5176	836.5177	-0.1	[|PE(40:6)|+2Na-H]+
Lung_MALDI	836.6105	836.6140	-3.5	[|PC(38:2)|+Na]+
Lung_MALDI	837.6802	837.6820	-1.8	[|SM(d42:1)|+Na]+
Lung_MALDI	838.5295	838.5333	-3.8	[|PE(40:5)|+2Na-H]+
Lung_MALDI	840.4329	840.4343	-1.4	[|PE(38:6)|+2K-H]+
Lung_MALDI	840.5461	840.5490	-2.9	[|PE(40:4)|+2Na-H]+
Lung_MALDI	842.4482	842.4499	-1.7	[|PE(38:5)|+2K-H]+
Lung_MALDI	844.4640	844.4656	-1.5	[|PE(38:4)|+2K-H]+
Lung_MALDI	844.5230	844.5253	-2.3	[|PC(38:6)|+K]+
Lung_MALDI	844.5230	844.5228	0.3	[|PE 42:8p|+2Na-H]+
Lung_MALDI	845.6980	845.6995	-1.5	[|TG(48:0)|+K]+
Lung_MALDI	846.5374	846.5384	-1.0	[|PE 42:7p|+2Na-H]+
Lung_MALDI	846.5374	846.5410	-3.6	[|PC(38:5)|+K]+
Lung_MALDI	848.5544	848.5566	-2.2	[|PC(38:4)|+K]+
Lung_MALDI	848.5544	848.5541	0.4	[|PE 42:6p|+2Na-H]+
Lung_MALDI	849.4406	849.4445	-3.8	[|PG(36:3)|+2K-H]+
Lung_MALDI	851.6385	851.6403	-1.8	[|SM(d42:2)|+K]+
Lung_MALDI	851.7091	851.7075	1.6	[|TG(48:0)|+2Na-H]+
Lung_MALDI	851.7091	851.7123	-3.2	[|TG(52:6)|+H]+
Lung_MALDI	851.7091	851.7099	-0.8	[|TG(50:3)|+Na]+
Lung_MALDI	852.5461	852.5490	-2.9	[|PC(38:5)|+2Na-H]+
Lung_MALDI	853.6541	853.6559	-1.9	[|SM(d42:1)|+K]+

Sample	Meas. *m/z*	Calc. *m/z*	Δm (mDa)	Tentative identification
Lung_MALDI	853.7240	853.7280	-4.0	[|TG(52:5)|+H]+
Lung_MALDI	853.7240	853.7256	-1.6	[|TG(50:2)|+Na]+
Lung_MALDI	854.5661	854.5670	-0.9	[|PC(40:7)|+Na]+
Lung_MALDI	854.5661	854.5694	-3.3	[|PC(42:10)|+H]+
Lung_MALDI	854.5661	854.5646	1.5	[|PC(38:4)|+2Na-H]+
Lung_MALDI	855.7388	855.7412	-2.4	[|TG(50:1)|+Na]+
Lung_MALDI	856.5242	856.5253	-1.1	[|PE(42:7)|+K]+
Lung_MALDI	856.5811	856.5827	-1.6	[|PC(40:6)|+Na]+
Lung_MALDI	856.5811	856.5803	0.8	[|PC(38:3)|+2Na-H]+
Lung_MALDI	858.4565	858.4564	0.1	[|Sulfatide(d34:0)|+2K-H]+
Lung_MALDI	860.6114	860.6116	-0.2	[|PC(38:1)|+2Na-H]+
Lung_MALDI	860.6114	860.6140	-2.6	[|PC(40:4)|+Na]+
Lung_MALDI	866.4677	866.4710	-3.3	[|PS(36:1)|+2K-H]+
Lung_MALDI	868.4642	868.4656	-1.3	[|PE(40:6)|+2K-H]+
Lung_MALDI	868.5231	868.5253	-2.2	[|PC(40:8)|+K]+
Lung_MALDI	869.6976	869.6995	-1.9	[|TG(50:2)|+K]+
Lung_MALDI	871.4256	871.4288	-3.2	[|PG(38:6)|+2K-H]+
Lung_MALDI	871.7145	871.7152	-0.6	[|TG(50:1)|+K]+
Lung_MALDI	872.5546	872.5566	-2.0	[|PC(40:6)|+K]+
Lung_MALDI	875.7100	875.7123	-2.3	[|TG(54:8)|+H]+
Lung_MALDI	875.7100	875.7099	0.1	[|TG(52:5)|+Na]+
Lung_MALDI	875.7100	875.7075	2.5	[|TG(50:2)|+2Na-H]+
Lung_MALDI	877.7241	877.7232	0.9	[|TG(50:1)|+2Na-H]+
Lung_MALDI	877.7241	877.7280	-3.9	[|TG(54:7)|+H]+
Lung_MALDI	877.7241	877.7256	-1.5	[|TG(52:4)|+Na]+
Lung_MALDI	879.7388	879.7388	0.0	[|TG(50:0)|+2Na-H]+
Lung_MALDI	879.7388	879.7412	-2.4	[|TG(52:3)|+Na]+
Lung_MALDI	880.4857	880.4864	-0.6	[|PE(44:12)|+2Na-H]+
Lung_MALDI	881.7538	881.7569	-3.0	[|TG(52:2)|+Na]+
Lung_MALDI	882.4792	882.4812	-2.0	[|PC(38:6)|+2K-H]+
Lung_MALDI	885.4664	885.4653	1.1	[|PG(42:11)|+2Na-H]+
Lung_MALDI	887.4472	887.4449	2.3	[|PI(32:0)|+2K-H]+
Lung_MALDI	888.4586	888.4554	3.2	[|PS(38:4)|+2K-H]+
Lung_MALDI	891.7033	891.7048	-1.5	[|22:1-Glc-cholesterol|+Na]+
Lung_MALDI	893.4107	893.4132	-2.5	[|PG(40:9)|+2K-H]+
Lung_MALDI	895.7137	895.7152	-1.4	[|TG(52:3)|+K]+
Lung_MALDI	897.7282	897.7308	-2.6	[|TG(52:2)|+K]+
Lung_MALDI	901.7242	901.7232	1.0	[|TG(52:3)|+2Na-H]+
Lung_MALDI	901.7242	901.7280	-3.8	[|TG(56:9)|+H]+
Lung_MALDI	901.7242	901.7256	-1.4	[|TG(54:6)|+Na]+
Lung_MALDI	903.7402	903.7388	1.4	[|TG(52:2)|+2Na-H]+
Lung_MALDI	903.7402	903.7412	-1.0	[|TG(54:5)|+Na]+
Lung_MALDI	903.7402	903.7436	-3.4	[|TG(56:8)|+H]+
Lung_MALDI	905.7554	905.7593	-3.9	[|TG(56:7)|+H]+
Lung_MALDI	905.7554	905.7545	0.9	[|TG(52:1)|+2Na-H]+
Lung_MALDI	905.7554	905.7569	-1.5	[|TG(54:4)|+Na]+
Lung_MALDI	907.7696	907.7725	-2.9	[|TG(54:3)|+Na]+

Sample	**Meas. *m/z***	**Calc. *m/z***	**Δm (mDa)**	**Tentative identification**
Lung_MALDI	908.4965	908.4969	-0.3	[|PC(40:7)|+2K-H]+
Lung_MALDI	913.4647	913.4605	4.2	[|PI(34:1)|+2K-H]+
Lung_MALDI	914.5282	914.5285	-0.3	[|PI-Cer(38:0)|+2K-H]+
Lung_MALDI	921.7301	921.7308	-0.7	[|TG(54:4)|+K]+
Lung_MALDI	931.5269	931.5283	-1.4	[|PI(38:4)|+2Na-H]+
Lung_MALDI	935.4447	935.4449	-0.1	[|PI(36:4)|+2K-H]+
Lung_MALDI	963.4744	963.4762	-1.7	[|PI(38:4)|+2K-H]+
Lung_MALDI	967.5060	967.5075	-1.5	[|PI(38:2)|+2K-H]+
Lung_MALDI	994.5865	994.5816	4.8	[|Sulfatide(d44:2)|+2K-H]+
Lung_NAPA	327.2271	327.2271	0.0	[|FA(18:1)|+2Na-H]+
Lung_NAPA	329.2429	329.2427	0.2	[|FA(18:0)|+2Na-H]+
Lung_NAPA	369.3519	369.3516	0.3	[|Cholesterol (-H2O)|+H]+
Lung_NAPA	457.1105	457.1119	-1.4	[|FMN|+H]+
Lung_NAPA	479.0940	479.0938	0.2	[|FMN|+Na]+
Lung_NAPA	500.2558	500.2539	1.9	[|Carnitine(18:2)|+2K-H]+
Lung_NAPA	501.0781	501.0758	2.3	[|FMN|+2Na-H]+
Lung_NAPA	516.2512	516.2487	2.5	[|LysoPE(18:2)|+K]+
Lung_NAPA	518.2669	518.2644	2.6	[|LysoPE(18:1)|+K]+
Lung_NAPA	526.2357	526.2332	2.5	[|Glycochenodeoxycholic acid|+2K-H]+
Lung_NAPA	544.2821	544.2800	2.1	[|LysoPE(20:2)|+K]+
Lung_NAPA	554.2663	554.2644	2.0	[|LysoPC(18:4)|+K]+
Lung_NAPA	558.2976	558.2957	2.0	[|LysoPC(18:2)|+K]+
Lung_NAPA	558.3503	558.3530	-2.7	[|LysoPE(22:1)|+Na]+
Lung_NAPA	562.3296	562.3270	2.6	[|LysoPC(18:0)|+K]+
Lung_NAPA	564.2510	564.2487	2.3	[|LysoPE(22:6)|+K]+
Lung_NAPA	568.2806	568.2800	0.5	[|LysoPE(22:4)|+K]+
Lung_NAPA	592.2816	592.2800	1.6	[|LysoPE(24:6)|+K]+
Lung_NAPA	602.3604	602.3583	2.1	[|LysoPE(24:1)|+K]+
Lung_NAPA	608.3132	608.3113	1.9	[|LysoPC(22:5)|+K]+
Lung_NAPA	610.3273	610.3270	0.4	[|LysoPC(22:4)|+K]+
Lung_NAPA	615.4950	615.4959	-0.9	[|DG(34:2)|+Na]+
Lung_NAPA	617.5109	617.5140	-3.0	[|DG(36:4)|+H]+
Lung_NAPA	617.5109	617.5116	-0.6	[|DG(34:1)|+Na]+
Lung_NAPA	631.4695	631.4698	-0.3	[|DG(34:2)|+K]+
Lung_NAPA	633.4856	633.4855	0.1	[|DG(34:1)|+K]+
Lung_NAPA	637.4795	637.4778	1.7	[|DG(34:2)|+2Na-H]+
Lung_NAPA	639.4950	639.4959	-0.9	[|DG(36:4)|+Na]+
Lung_NAPA	639.4950	639.4935	1.5	[|DG(34:1)|+2Na-H]+
Lung_NAPA	641.5106	641.5116	-1.0	[|DG(36:3)|+Na]+
Lung_NAPA	643.5263	643.5272	-0.9	[|DG(36:2)|+Na]+
Lung_NAPA	657.4862	657.4855	0.7	[|DG(36:3)|+K]+
Lung_NAPA	659.5016	659.5011	0.5	[|DG(36:2)|+K]+
Lung_NAPA	666.4817	666.4833	-1.6	[|CerP(d36:2)|+Na]+
Lung_NAPA	667.5251	667.5272	-2.1	[|DG(38:4)|+Na]+
Lung_NAPA	667.5251	667.5248	0.3	[|DG(36:1)|+2Na-H]+
Lung_NAPA	669.4459	669.4466	-0.7	[|PA(32:1)|+Na]+
Lung_NAPA	669.4459	669.4490	-3.1	[|PA(34:4)|+H]+

Sample	Meas. *m/z*	Calc. *m/z*	Δm (mDa)	Tentative identification
Lung_NAPA	670.6103	670.6109	-0.6	[|Cer(d42:2)|+Na]+
Lung_NAPA	681.4848	681.4855	-0.7	[|DG(38:5)|+K]+
Lung_NAPA	682.4564	682.4572	-0.9	[|CerP(d36:2)|+K]+
Lung_NAPA	688.4626	688.4652	-2.6	[|CerP(d36:2)|+2Na-H]+
Lung_NAPA	691.4275	691.4285	-1.0	[|PA(32:1)|+2Na-H]+
Lung_NAPA	691.4275	691.4309	-3.4	[|PA(34:4)|+Na]+
Lung_NAPA	693.4424	693.4442	-1.8	[|PA(32:0)|+2Na-H]+
Lung_NAPA	697.4766	697.4779	-1.3	[|PA(34:1)|+Na]+
Lung_NAPA	710.3550	710.3560	-1.0	[|PE(28:1)|+2K-H]+
Lung_NAPA	713.4506	713.4518	-1.2	[|PA(34:1)|+K]+
Lung_NAPA	719.4581	719.4598	-1.7	[|PA(34:1)|+2Na-H]+
Lung_NAPA	721.4768	721.4779	-1.0	[|PA(36:3)|+Na]+
Lung_NAPA	721.4768	721.4803	-3.4	[|PA(38:6)|+H]+
Lung_NAPA	721.4768	721.4755	1.4	[|PA(34:0)|+2Na-H]+
Lung_NAPA	722.5522	722.5541	-2.0	[|HexCer(d34:1)|+Na]+
Lung_NAPA	723.4923	723.4935	-1.2	[|PA(36:2)|+Na]+
Lung_NAPA	723.4923	723.4959	-3.6	[|PA(38:5)|+H]+
Lung_NAPA	725.5549	725.5568	-1.9	[|SM(d34:1)|+Na]+
Lung_NAPA	728.5177	728.5201	-2.4	[|PC(30:0)|+Na]+
Lung_NAPA	731.4053	731.4049	0.5	[|PA(36:6)|+K]+
Lung_NAPA	733.4169	733.4205	-3.6	[|PA(36:5)|+K]+
Lung_NAPA	736.4834	736.4864	-3.0	[|PE(32:0)|+2Na-H]+
Lung_NAPA	737.4519	737.4518	0.1	[|PA(36:3)|+K]+
Lung_NAPA	739.4105	739.4101	0.4	[|DG(40:9)|+2K-H]+
Lung_NAPA	739.4660	739.4675	-1.5	[|PA(36:2)|+K]+
Lung_NAPA	740.4046	740.4030	1.6	[|PE(30:0)|+2K-H]+
Lung_NAPA	741.4422	741.4442	-1.9	[|PA(36:4)|+2Na-H]+
Lung_NAPA	741.5990	741.6004	-1.3	[|TG(42:2)|+Na]+
Lung_NAPA	742.5336	742.5357	-2.1	[|PE(34:0)|+Na]+
Lung_NAPA	743.4600	743.4598	0.2	[|PA(36:3)|+2Na-H]+
Lung_NAPA	743.4600	743.4622	-2.2	[|PA(38:6)|+Na]+
Lung_NAPA	745.4745	745.4779	-3.4	[|PA(38:5)|+Na]+
Lung_NAPA	745.4745	745.4755	-1.0	[|PA(36:2)|+2Na-H]+
Lung_NAPA	747.4899	747.4911	-1.2	[|PA(36:1)|+2Na-H]+
Lung_NAPA	747.4899	747.4935	-3.6	[|PA(38:4)|+Na]+
Lung_NAPA	747.4899	747.4879	2.0	[|CE(20:5)|+2K-H]+
Lung_NAPA	748.5824	748.5851	-2.7	[|PE(36:0)|+H]+
Lung_NAPA	751.4063	751.4077	-1.4	[|PA(34:1)|+2K-H]+
Lung_NAPA	753.5855	753.5881	-2.6	[|SM(d36:1)|+Na]+
Lung_NAPA	754.5334	754.5357	-2.4	[|PC(32:1)|+Na]+
Lung_NAPA	756.4927	756.4940	-1.4	[|PE(34:1)|+K]+
Lung_NAPA	757.4182	757.4205	-2.3	[|PA(38:7)|+K]+
Lung_NAPA	758.5081	758.5097	-1.6	[|PE(34:0)|+K]+
Lung_NAPA	759.4337	759.4362	-2.4	[|PA(38:6)|+K]+
Lung_NAPA	763.4652	763.4675	-2.2	[|PA(38:4)|+K]+
Lung_NAPA	764.5160	764.5177	-1.7	[|PE(34:0)|+2Na-H]+
Lung_NAPA	766.4182	766.4186	-0.4	[|PE(32:1)|+2K-H]+

Sample	Meas. *m/z*	Calc. *m/z*	Δm (mDa)	Tentative identification
Lung_NAPA	766.4182	766.4147	3.6	[|Sulfatide(d30:2)|+2Na-H]+
Lung_NAPA	767.4573	767.4598	-2.5	[|PA(38:5)|+2Na-H]+
Lung_NAPA	768.4883	768.4915	-3.2	[|PE 36:4p|+2Na-H]+
Lung_NAPA	769.4729	769.4755	-2.6	[|PA(38:4)|+2Na-H]+
Lung_NAPA	771.4946	771.4911	3.4	[|PA(38:3)|+2Na-H]+
Lung_NAPA	771.4946	771.4935	1.0	[|PA(40:6)|+Na]+
Lung_NAPA	772.5229	772.5252	-2.3	[|PE 38:5p|+Na]+
Lung_NAPA	772.5229	772.5228	0.1	[|PE 36:2p|+2Na-H]+
Lung_NAPA	775.4042	775.4077	-3.5	[|PA(36:3)|+2K-H]+
Lung_NAPA	777.4233	777.4234	-0.1	[|PA(36:2)|+2K-H]+
Lung_NAPA	778.4217	778.4186	3.1	[|PC(30:2)|+2K-H]+
Lung_NAPA	778.4752	778.4784	-3.2	[|PE(36:4)|+K]+
Lung_NAPA	780.4902	780.4940	-3.8	[|PE(36:3)|+K]+
Lung_NAPA	780.5481	780.5514	-3.3	[|PC(34:2)|+Na]+
Lung_NAPA	782.5649	782.5670	-2.2	[|PC(34:1)|+Na]+
Lung_NAPA	784.5219	784.5253	-3.4	[|PE(36:1)|+K]+
Lung_NAPA	786.3897	786.3873	2.4	[|PE(34:5)|+2K-H]+
Lung_NAPA	790.4205	790.4186	1.9	[|PE(34:3)|+2K-H]+
Lung_NAPA	790.5311	790.5333	-2.3	[|PE(36:1)|+2Na-H]+
Lung_NAPA	791.4635	791.4598	3.7	[|PA(40:7)|+2Na-H]+
Lung_NAPA	792.4320	792.4343	-2.2	[|PE(34:2)|+2K-H]+
Lung_NAPA	794.4491	794.4460	3.1	[|Sulfatide(d32:2)|+2Na-H]+
Lung_NAPA	794.4491	794.4499	-0.8	[|PE(34:1)|+2K-H]+
Lung_NAPA	794.5032	794.5071	-3.9	[|PE 38:5p|+2Na-H]+
Lung_NAPA	794.6091	794.6117	-2.5	[|HexCer(d38:1(2OH))|+Na]+
Lung_NAPA	796.4646	796.4656	-1.0	[|PE(34:0)|+2K-H]+
Lung_NAPA	796.4646	796.4616	3.0	[|Sulfatide(d32:1)|+2Na-H]+
Lung_NAPA	796.5206	796.5228	-2.1	[|PE 38:4p|+2Na-H]+
Lung_NAPA	798.5389	798.5410	-2.1	[|PC(34:1)|+K]+
Lung_NAPA	798.5389	798.5408	-2.0	[|PE 40:6p|+Na]+
Lung_NAPA	798.5389	798.5384	0.4	[|PE 38:3p|+2Na-H]+
Lung_NAPA	799.6755	799.6786	-3.2	[|TG(46:1)|+Na]+
Lung_NAPA	801.4211	801.4234	-2.3	[|PA(38:4)|+2K-H]+
Lung_NAPA	801.6925	801.6943	-1.8	[|TG(46:0)|+Na]+
Lung_NAPA	804.4903	804.4940	-3.7	[|PE(38:5)|+K]+
Lung_NAPA	804.5483	804.5490	-0.7	[|PC(34:1)|+2Na-H]+
Lung_NAPA	804.5483	804.5514	-3.1	[|PC(36:4)|+Na]+
Lung_NAPA	804.6324	804.6324	0.0	[|HexCer(d18:2/22:0)|+Na]+
Lung_NAPA	806.5069	806.5097	-2.8	[|PE(38:4)|+K]+
Lung_NAPA	806.6459	806.6480	-2.1	[|HexCer(d18:1/22:0)|+Na]+
Lung_NAPA	808.5808	808.5827	-1.8	[|PC(36:2)|+Na]+
Lung_NAPA	809.6485	809.6507	-2.2	[|SM(d40:1)|+Na]+
Lung_NAPA	810.5889	810.5856	3.3	[|HexCer(d38:1(2OH))|+K]+
Lung_NAPA	813.6007	813.5980	2.7	[|TG(46:5)|+2Na-H]+
Lung_NAPA	815.4651	815.4622	2.8	[|PA(44:12)|+Na]+
Lung_NAPA	815.6533	815.6526	0.8	[|TG(46:1)|+K]+
Lung_NAPA	816.4318	816.4343	-2.5	[|PE(36:4)|+2K-H]+

Sample	Meas. *m/z*	Calc. *m/z*	Δm (mDa)	Tentative identification
Lung_NAPA	817.6667	817.6682	-1.5	[|TG(46:0)|+K]+
Lung_NAPA	818.5640	818.5646	-0.6	[|PE(38:1)|+2Na-H]+
Lung_NAPA	818.5640	818.5670	-3.0	[|PE(40:4)|+Na]+
Lung_NAPA	820.4635	820.4656	-2.0	[|PE(36:2)|+2K-H]+
Lung_NAPA	820.5207	820.5228	-2.0	[|PE 40:6p|+2Na-H]+
Lung_NAPA	822.4802	822.4812	-1.0	[|PE(36:1)|+2K-H]+
Lung_NAPA	822.4802	822.4773	2.9	[|Sulfatide(d34:2)|+2Na-H]+
Lung_NAPA	822.5359	822.5384	-2.5	[|PE 40:5p|+2Na-H]+
Lung_NAPA	822.6411	822.6430	-1.9	[|HexCer(t40:1)|+Na]+
Lung_NAPA	824.5530	824.5565	-3.5	[|PE 42:7p|+Na]+
Lung_NAPA	824.5530	824.5541	-1.0	[|PE 40:4p|+2Na-H]+
Lung_NAPA	824.5530	824.5566	-3.6	[|PC(36:2)|+K]+
Lung_NAPA	825.6924	825.6943	-1.9	[|TG(48:2)|+Na]+
Lung_NAPA	827.4359	827.4390	-3.1	[|PA(40:5)|+2K-H]+
Lung_NAPA	827.7082	827.7099	-1.8	[|TG(48:1)|+Na]+
Lung_NAPA	828.4910	828.4940	-3.0	[|PE(40:7)|+K]+
Lung_NAPA	829.7237	829.7256	-1.8	[|TG(48:0)|+Na]+
Lung_NAPA	830.6460	830.6456	0.4	[|HexCer(d40:0)|+2Na-H]+
Lung_NAPA	832.5214	832.5253	-3.9	[|PE(40:5)|+K]+
Lung_NAPA	832.5802	832.5827	-2.5	[|PC(38:4)|+Na]+
Lung_NAPA	832.5802	832.5803	-0.1	[|PC(36:1)|+2Na-H]+
Lung_NAPA	832.6614	832.6637	-2.2	[|HexCer(d42:2)|+Na]+
Lung_NAPA	834.5379	834.5410	-3.1	[|PE(40:4)|+K]+
Lung_NAPA	834.6764	834.6793	-3.0	[|HexCer(d42:1)|+Na]+
Lung_NAPA	838.5108	838.5125	-1.7	[|PC(34:0)|+2K-H]+
Lung_NAPA	838.5108	838.5148	-4.0	[|PE 42:8p|+K]+
Lung_NAPA	838.6146	838.6168	-2.2	[|PI-Cer(38:0)|+H]+
Lung_NAPA	838.6146	838.6169	-2.3	[|HexCer(t40:1)|+K]+
Lung_NAPA	839.7031	839.7001	3.1	[|SM(d44:3)|+H]+
Lung_NAPA	840.4338	840.4343	-0.5	[|PE(38:6)|+2K-H]+
Lung_NAPA	841.6669	841.6682	-1.3	[|TG(48:2)|+K]+
Lung_NAPA	842.4479	842.4499	-2.0	[|PE(38:5)|+2K-H]+
Lung_NAPA	843.6822	843.6839	-1.6	[|TG(48:1)|+K]+
Lung_NAPA	844.4643	844.4656	-1.2	[|PE(38:4)|+2K-H]+
Lung_NAPA	845.6983	845.6995	-1.2	[|TG(48:0)|+K]+
Lung_NAPA	848.4908	848.4929	-2.1	[|Sulfatide(d36:3)|+2Na-H]+
Lung_NAPA	848.5534	848.5541	-0.7	[|PE 42:6p|+2Na-H]+
Lung_NAPA	848.5534	848.5566	-3.3	[|PC(38:4)|+K]+
Lung_NAPA	848.6590	848.6586	0.4	[|HexCer(d42:2(2OH))|+Na]+
Lung_NAPA	849.6915	849.6943	-2.8	[|TG(50:4)|+Na]+
Lung_NAPA	849.6915	849.6919	-0.4	[|TG(48:1)|+2Na-H]+
Lung_NAPA	850.6763	850.6743	2.1	[|HexCer(d42:1(2OH))|+Na]+
Lung_NAPA	851.7072	851.7075	-0.3	[|TG(48:0)|+2Na-H]+
Lung_NAPA	851.7072	851.7099	-2.7	[|TG(50:3)|+Na]+
Lung_NAPA	853.7237	853.7256	-1.9	[|TG(50:2)|+Na]+
Lung_NAPA	854.5075	854.5097	-2.2	[|PE(42:8)|+K]+
Lung_NAPA	855.7392	855.7412	-2.1	[|TG(50:1)|+Na]+

Sample	Meas. *m/z*	Calc. *m/z*	Δm (mDa)	Tentative identification
Lung_NAPA	856.5238	856.5253	-1.5	[|PE(42:7)|+K]+
Lung_NAPA	858.4550	858.4564	-1.4	[|Sulfatide(d34:0)|+2K-H]+
Lung_NAPA	863.6995	863.6977	1.8	[|SM(d44:2)|+Na]+
Lung_NAPA	865.6671	865.6682	-1.1	[|TG(50:4)|+K]+
Lung_NAPA	865.7130	865.7133	-0.3	[|SM(d44:1)|+Na]+
Lung_NAPA	866.4747	866.4710	3.7	[|PS(36:1)|+2K-H]+
Lung_NAPA	866.6486	866.6482	0.4	[|HexCer(d42:1(2OH))|+K]+
Lung_NAPA	866.6486	866.6481	0.5	[|PI-Cer(40:0)|+H]+
Lung_NAPA	868.4628	868.4656	-2.7	[|PE(40:6)|+2K-H]+
Lung_NAPA	869.6974	869.6995	-2.1	[|TG(50:2)|+K]+
Lung_NAPA	871.4310	871.4288	2.1	[|PG(38:6)|+2K-H]+
Lung_NAPA	871.7135	871.7152	-1.7	[|TG(50:1)|+K]+
Lung_NAPA	872.4962	872.4969	-0.6	[|PE(40:4)|+2K-H]+
Lung_NAPA	875.7083	875.7075	0.7	[|TG(50:2)|+2Na-H]+
Lung_NAPA	875.7083	875.7123	-4.1	[|TG(54:8)|+H]+
Lung_NAPA	875.7083	875.7099	-1.7	[|TG(52:5)|+Na]+
Lung_NAPA	877.7235	877.7256	-2.0	[|TG(52:4)|+Na]+
Lung_NAPA	877.7235	877.7232	0.4	[|TG(50:1)|+2Na-H]+
Lung_NAPA	879.4530	879.4573	-4.3	[|PG(42:11)|+K]+
Lung_NAPA	879.7388	879.7412	-2.4	[|TG(52:3)|+Na]+
Lung_NAPA	879.7388	879.7388	0.0	[|TG(50:0)|+2Na-H]+
Lung_NAPA	881.7538	881.7569	-3.1	[|TG(52:2)|+Na]+
Lung_NAPA	884.6038	884.6070	-3.1	[|LacCer(d34:1)|+Na]+
Lung_NAPA	885.4656	885.4653	0.3	[|PG(42:11)|+2Na-H]+
Lung_NAPA	887.4810	887.4810	0.1	[|PG(42:10)|+2Na-H]+
Lung_NAPA	891.6817	891.6839	-2.1	[|TG(52:5)|+K]+
Lung_NAPA	895.7117	895.7152	-3.4	[|TG(52:3)|+K]+
Lung_NAPA	897.7278	897.7308	-3.0	[|TG(52:2)|+K]+
Lung_NAPA	901.7231	901.7232	-0.1	[|TG(52:3)|+2Na-H]+
Lung_NAPA	901.7231	901.7256	-2.5	[|TG(54:6)|+Na]+
Lung_NAPA	903.7399	903.7388	1.1	[|TG(52:2)|+2Na-H]+
Lung_NAPA	903.7399	903.7412	-1.4	[|TG(54:5)|+Na]+
Lung_NAPA	903.7399	903.7436	-3.8	[|TG(56:8)|+H]+
Lung_NAPA	905.7553	905.7593	-3.9	[|TG(56:7)|+H]+
Lung_NAPA	905.7553	905.7545	0.9	[|TG(52:1)|+2Na-H]+
Lung_NAPA	905.7553	905.7569	-1.5	[|TG(54:4)|+Na]+
Lung_NAPA	907.6761	907.6788	-2.7	[|22:1-Glc-cholesterol|+K]+
Lung_NAPA	907.7696	907.7725	-2.9	[|TG(54:3)|+Na]+
Lung_NAPA	911.4444	911.4449	-0.5	[|PI(34:2)|+2K-H]+
Lung_NAPA	912.4550	912.4554	-0.3	[|PS(40:6)|+2K-H]+
Lung_NAPA	915.4736	915.4762	-2.6	[|PI(34:0)|+2K-H]+
Lung_NAPA	917.4097	917.4132	-3.4	[|PG(42:11)|+2K-H]+
Lung_NAPA	921.4881	921.4890	-0.9	[|PI(38:6)|+K]+
Lung_NAPA	923.7434	923.7465	-3.1	[|TG(54:3)|+K]+
Lung_NAPA	929.7552	929.7545	0.7	[|TG(54:3)|+2Na-H]+
Lung_NAPA	929.7552	929.7593	-4.1	[|TG(58:9)|+H]+
Lung_NAPA	929.7552	929.7569	-1.7	[|TG(56:6)|+Na]+

Sample	**Meas. *m/z***	**Calc. *m/z***	**Δm (mDa)**	**Tentative identification**
Lung_NAPA	931.7690	931.7725	-3.5	[|TG(56:5)|+Na]+
Lung_NAPA	931.7690	931.7701	-1.1	[|TG(54:2)|+2Na-H]+
Lung_NAPA	933.7857	933.7858	-0.1	[|TG(54:1)|+2Na-H]+
Lung_NAPA	933.7857	933.7882	-2.5	[|TG(56:4)|+Na]+
Lung_NAPA	935.7992	935.8038	-4.6	[|TG(56:3)|+Na]+
Lung_NAPA	936.5006	936.5034	-2.8	[|Sulfatide(d40:3)|+2K-H]+
Lung_NAPA	940.4833	940.4867	-3.4	[|PS(42:6)|+2K-H]+
Lung_NAPA	945.7283	945.7308	-2.5	[|TG(56:6)|+K]+
Lung_NAPA	947.7438	947.7465	-2.6	[|TG(56:5)|+K]+
Lung_NAPA	959.4494	959.4449	4.5	[|PI(38:6)|+2K-H]+
Lung_NAPA	963.4742	963.4762	-2.0	[|PI(38:4)|+2K-H]+
Lung_NAPA	964.6507	964.6494	1.3	[|Sulfatide(d44:1)|+2Na-H]+
Lung_NAPA	968.6965	968.7009	-4.4	[|LacCer(d40:1)|+Na]+
Lung_NAPA	991.5117	991.5075	4.2	[|PI(40:4)|+2K-H]+
Lung_NAPA	994.7138	994.7165	-2.7	[|LacCer(d42:2)|+Na]+